

Review

Recent Advances in the Application of Metal–Organic Frameworks for Polymerization and Oligomerization Reactions

Fangyu Ren ¹  and Pengfei Ji ^{2,*} 

¹ State Key Laboratory and Institute of Elemento–Organic Chemistry, College of Chemistry, Nankai University, Tianjin 300071, China; 2120180918@mail.nankai.edu.cn

² Department of Chemistry, University of California, Berkeley, CA 94720, USA

* Correspondence: jipengfei@berkeley.edu

Received: 17 November 2020; Accepted: 7 December 2020; Published: 9 December 2020



Abstract: Polymers have become one of the major types of materials that are essential in our daily life. The controlled synthesis of value-added polymers with unique mechanical and chemical properties have attracted broad research interest. Metal–organic framework (MOF) is a class of porous material with immense structural diversity which offers unique advantages for catalyzing polymerization and oligomerization reactions including the uniformity of the catalytic active site, and the templating effect of the nano-sized channels. We summarized in this review the important recent progress in the field of MOF-catalyzed and MOF-templated polymerizations, to reveal the chemical principle and structural aspects of these systems and hope to inspire the future design of novel polymerization systems with improved activity and specificity.

Keywords: catalysis; metal–organic frameworks; polymer; polymerization; ribosome

1. Introduction

Metal–organic frameworks (MOFs), constructed from inorganic nodes and organic linkers, have emerged as a new class of hybrid materials ordered into two- or three-dimensional network [1,2]. MOFs with permanent porosity were first discovered at the end of the 20th century and have attracted broad research interest over the past 2–3 decades, owing to their distinctive features including their porosity, tunable function, and structural diversity [3–5], MOFs have unfolded enormous potential for application in gas storage and separation [6–8], sensing [9–11], drug delivery [12–14], sustainable energy [15–17], as well as catalysis [18–20].

Prior to the mid-1990s, researchers mainly focused on two types of porous materials, either purely inorganic materials or carbon materials [21]. MOF is an unprecedented class of porous material that combines the feature of both of the two types. Similar to zeolites, MOFs are generally synthesized through hydrothermal or solvothermal methods, which allow for steady nucleation of crystal seed from hot solutions [22]. However, MOFs utilize organic linkers to bridge metal clusters and form two or three dimensional lattice [23], which offer greatly increase structural diversity than classical porous materials. Zeolites have found broad application for catalysis in chemical industry owing to its uniform porosity, but the types of reactions are limited to acid-catalyzed reactions [24]. MOFs also feature uniform pores that preferentially interact with substrates with the proper shapes and sizes [25]. Moreover, both the inorganic node and organic linker allows for the introduction of various functional group [26]. As a result, the catalytic function of MOFs are far beyond Brønsted or Lewis acidity [27]. The structure and function for certain family of MOFs can even be customized and tailor-made [28,29].

These advantages of MOF catalysts have offered great promise for their application in polymerization, which is an indispensable part of chemical industry [30–32]. Uemura et al. [33] reported

the use of MOF to template the free radical polymerization of styrene (St) in 2005. Large numbers of researchers have been especially interested in using MOFs to catalyze the polymerization reaction [34–36]. Classical catalysts for olefin polymerization are mainly heterogeneous catalysts such as the Ziegler–Natta catalyst, which is favored for their low-cost, thermal stability, reusability, and ease for separation from products [37–39]. Heterogeneous catalysts have developed rapidly in the past several decades and have shown significant strength in controlling the branching and tacticity of polymers [40–42]. One remaining challenge is to build a catalyst system that can control the polymerization process across the length of multiple monomers to achieve unique morphology, regioselectivity, and even sequence specificity [43–45]. This level of control would allow the synthesis of polymers with greatly enhanced structural complexity, to better fit our need in developing advanced biomedical materials.

This level of control over precise polymerization is constantly engaged in the biological synthesis of macromolecules catalyzed by enzymes and ribosomes [46–48]. The precise chemoselectivity, regioselectivity, and stereoselectivity allows for the conversion of inanimate substances into biopolymers with sophisticated functions. Ribosomes are known as the molecular machinery for protein synthesis in cells [49]. During the normal operation of ribosomes, the efficiency and accuracy of each reaction process are related to the molecular recognition mechanism of mRNA, tRNA, and various translation factors interacting with ribosomes [50–52]. Compared to classical heterogeneous and homogeneous polymerization catalysts, which lack sufficient structural complexity, MOFs have greater potential for mimicking biological systems to achieve fully controlled polymerizations.

This review summarizes the recent advances in MOF-catalyzed polymerization, and grouped literature in two main sections, including the unique MOF-based catalysts for polymerization without templating effect (Figure 1A), and MOF-controlled polymerization through templating effect (Figure 1B).

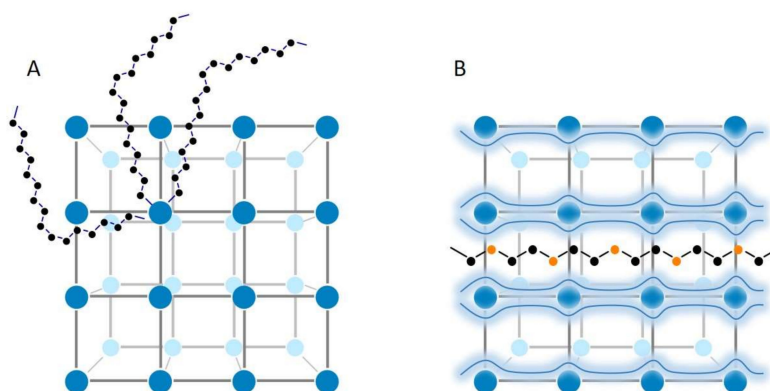


Figure 1. (A) Metal–organic frameworks (MOFs) as catalysts for polymerization. (B) MOFs as templates for polymerization.

2. MOF-Based Catalysts for Polymerization and Oligomerization Reactions

Although all parts of MOFs may be catalytically active through modification, inorganic nodes as a structurally monodisperse and well-defined transition metal catalytic platform, have attracted increasing attention. Notably, these secondary building units (SBUs) or clusters go through cation exchange with structure retention, so transition metals can be introduced to adjust their catalytic performance to achieve the desired application for catalysis. Compared to the strategy of physically including catalytic complexes, it is easier to achieve catalytic polymerization with precise polymer structure and stable morphology through the method of node modification. The incorporation of catalytic metal centers could also be achieved through covalent linking to organic linkers.

2.1. MOF-Catalyzed Polymerization through Organometallic Mechanism

2.1.1. Zirconium-Based MOF Catalysts

Farha and co-workers developed a Hf-NU1000-ZrBn catalyst (Figure 2A) [53] using well-defined mesoporous Hf-NU-1000 as a scaffold, and adding organozirconium complex as a single-site zirconium benzyl catalytic center with highly electrophilicity. The synthesized MOF catalysts are active for the homopolymerization of ethylene and stereospecific polymerization 1-hexene. In addition, as a single-component catalyst, there is no need to add activators or co-catalysts in the catalytic process to generate coordination-unsaturated Zr center. The calculated CM5 charges and natural population analysis calculations of species C revealed that the interaction between Zr and MOF SBU might be more ionic than covalent, promoting the coordination of monomers to the electrophilic d^0 Zr center.

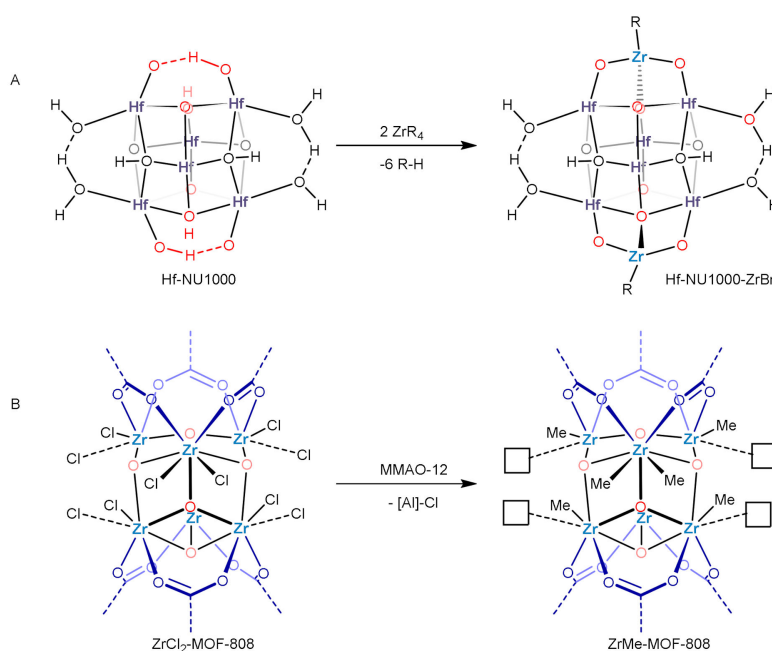


Figure 2. (A) Synthesis and structure of Hf-NU1000-ZrBn catalyst. (B) Synthesis and structure of ZrMe-BTC catalyst. Blank square indicates open coordination around zirconium.

In 2017, Lin and coworkers [54] developed a novel strategy to build multinuclear Zr catalysts with unique electronic and steric properties for olefin polymerization. The catalyst is prepared by exchanging the water and hydroxide group on the metal nodes with chlorides, followed by alkylation with MMAO-12 to obtain ZrMe-BTC (Figure 2B). ZrMe-BTC is proposed to contain one open coordination site around zirconium which allows for the coordination of alkene and subsequent migratory insertion to achieve polymerization. It is worth noting that the MOFs still maintained efficient activity at high pressures and high temperatures up to 140 °C.

2.1.2. Nickel-Based MOF Catalysts

Canivet et al. [55] proposed a novel post-synthetic functionalization of MOF linkers to generate nickel-based MOF catalysts. Under mild conditions, organometallic nickel catalyst was fixed in the cavity of the MOF in one pot. This method avoids the interaction of molecular catalysts with another active site in close proximity, or with the surface of metal oxides [56]. They functionalized 2-aminoterephthalate with pyridine carboxaldehyde to generate N,N-chelating pyridine methanimino group in the MOF cavity. In order to avoid the coordination of pyridine carboxaldehyde with the open site on Fe₃(μ₃-O) SBU, the pyridine carboxaldehyde was first coordinated with nickel, followed by

condensation with amino groups on the MOF linker (Figure 3A). The prepared nickel-based MOF catalyst showed high activity and selectivity for the dimerization of ethylene.

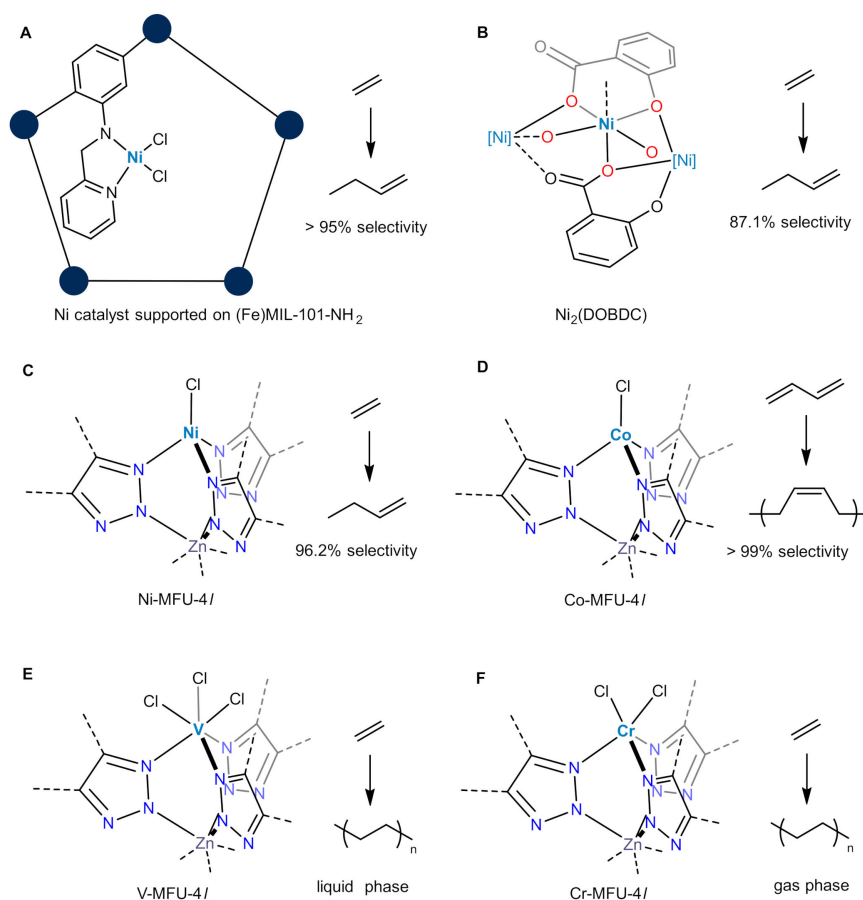


Figure 3. Proposed structure in literature for single-site metal catalysts for olefin polymerization, including (A) Ni catalyst supported on Fe-MIL-101-NH₂, (B) Ni₂(DOBDC), (C) Ni-MFU-4l, (D) Co-MFU-4l, (E) V-MFU-4l, and (F) Cr-MFU-4l.

Through previous research, nickel-doped zeolite can catalyze the polymerization of propylene in the gas phase. However, both the activity of the catalyst and the degree of branching of the resulting polymer are affected by the porous space near the Ni²⁺ site. Catalysts with high activity tend to give high branching of the oligomerization product. One way to produce linear oligomers with low-branching is to confine the reaction in narrower channel, at the cost of reduced reaction rate [57]. In view of the shortcomings of nickel-exchanged aluminosilicate materials, Bell and Long et al. [58] developed two metal–organic frameworks, namely Ni₂(dobdc) and Ni₂(dobpdc) (Figure 3B). Ni²⁺ is incorporated into the unique environment provided by the framework to maintain the high selectivity of propylene oligomerization reaction in the gas phase with high catalytic activity. The produced linear oligomers of propylene are potentially suitable for applications as diesel fuel and detergent.

Another type of nickel MOF was reported in 2016 by Dincă and co-workers [59,60] to catalyze the dimerization of ethylene with high efficiency and selectivity toward 1-butene. Conventional heterogeneous catalysts contained diverse types of active species, which made it difficult to control the dimerization of ethylene [61]. Therefore, mainly homogeneous catalysts were generally used to achieve ethylene dimerization with high selectivity. The coordination mode of Zn²⁺ and the surrounding bond angles and lengths are similar to those of the molecular analogue [Tp^{Mes}Ni]⁺ complexes, which is a proven catalyst for ethylene dimerization (Figure 3C). One limitation with this MOF catalyst is the low thermal stability, indicated by the marked drop of reaction rate at 50 °C.

The research group also used density functional theory calculations, isotope labeling and mechanistic probes to jointly prove the mechanism of NiMFU-4l catalyzing the dimerization of ethylene. It is proved that operates through the Cossee–Arlman mechanism, which is also in line with the characteristics of post-transition metal catalysts.

Afterward, Dincă group reported a nickel-CFA-1 which can replace nickel-MFU-4l in industry to catalyze ethylene dimerization with longer activity and lower cost [62]. The nickel-CFA-1 (Figure 3D) activated by MMAO-12 achieved a turnover frequency of 37,100 h⁻¹ and a 1-butene selectivity of 87.1% as well as maintained high activity after 12 h. Furthermore, the performance of the Nickel-CFA-1 was scaled up in a one-liter semibatch reactor, it still showed great activity, affordability, and selectivity.

2.1.3. Cobalt-Based MOF Catalysts

In 2017, Dincă group [63] reported Co-MFU-4l as a heterogeneous catalyst with high stereoselectivity (>99% 1,4-*cis*) for the production of 1,3-butadiene (Figure 3D). The low polydispersity (PDI ≈ 2) of the polymer, the easy recovery and low leaching of the catalyst indicate that the material is a type of single-site heterogeneous catalyst with anti-interference structure. Co-MFU-4l was further characterized by X-ray absorption spectroscopy to validate the coordination of Co(II) center to the tridentate N-donor ligands on the MOF SBU. The authors also synthesized a soluble cobalt complex with similar structure to Co-MFU-4l to provide rational understanding of the reaction mechanism in solution phase. TpMesCoCl was synthesized as a close structural analogue accessible by metal metathesis with TpMesTi. The mechanism for stereoselective polymerization and decomposition pathway of the catalyst was well understood by studying the small molecule analogue.

2.1.4. Vanadium-Based MOF Catalysts

Vanadium catalysts have found little application in large-scale polymerizations in industry for their poor stability, which leads to rapid deactivation during reaction process. However, vanadium metal catalysts have high stereoselectivity in olefin polymerization. Dincă et al. [64] introduced vanadium into MFU-4l through cation exchange to obtain a stable vanadium-based MOF catalyst that maintains high activity for more than 24 h (Figure 3E). The catalytic polymerization proceeded with high turn-over frequency up to 148,000 h⁻¹ and the obtained polyethylene featured low polydispersity (PDI ≈ 3).

2.1.5. Chromium-Based MOF Catalysts

In industrial applications, chromium-based catalysts were used for polymerizing ethylene with exceptional reactivity. But knowledge in the structure of the active catalysts and understanding of reaction mechanism is still lacking. Therefore, Dincă and co-workers [65] synthesized a MOF catalyst, through the exchange of inorganic nodes of MFU-4l with Cr(III) salt to obtain Cr(III)-MFU-4l (Figure 3F). No co-catalyst or solvent is needed in the catalytic process. The produced polyethylene has a low polydispersity index (1.6) and a free-flowing granular morphology. The MOF catalyst in gas phase polymerization has higher activity and lifespan than the slurry-phase method. The reaction time was extended to 24 h with no obvious deactivation.

2.1.6. Lanthanide-Based MOF Catalysts

Studies have shown that neodymium-based MOF materials are able to effectively catalyze the polymerization of isoprene [66]. Loiseau et al. [67] used different carboxylic acids as linkers to hydrothermally synthesize four kinds of neodymium-based MOFs, solved the structure of the MOFs with single-crystal X-ray diffraction. The water-free Nd(2,6-ndc)(form) (3) and Nd(form)₃ (4) combined with aluminoxanes polymerize isoprene into *cis*-polyisoprene with high conversion (up to 88.7%).

In 2015, Visseaux et al. [68] doped another lanthanide element to the lanthanide MOF, either europium or terbium, to introduce luminescence to the polymerization product. By changing the ratio of Nd and Ln (Ln = Eu or Tb), the polymerization of isoprene leads to products with varied

stereoselectivities [69]. In addition, luminescent cis-1,4 polyisoprenes were produced when $\text{Nd}(\text{form})_3$ and $\text{Ln}(\text{form})_3$ added together as the catalyst (Figure 4).

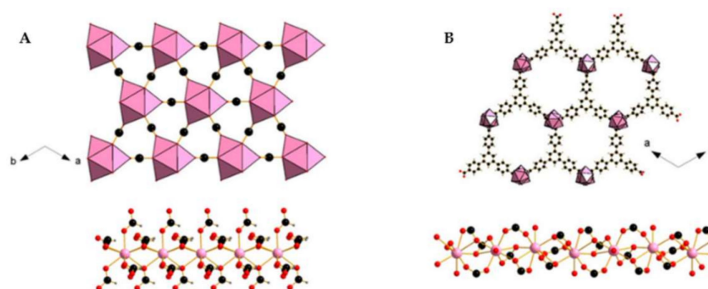


Figure 4. The structure of $\text{Nd}(\text{form})_3$ (A) and MIL-103(Nd) (B) pre-catalysts for polymerization [68]. Copyright 2016, American Chemical Society.

2.2. MOF-Catalyzed Polymerization through Radical-Chain Mechanism

2.2.1. Titanium-Based MOFs as Photocatalysts

Nguyen et al. [70,71] introduced a titanium unit as inorganic node to synthesize MOF-901, which can polymerize methyl methacrylate under visible light (Figure 5). The polymerization product has a low PDI of 1.6 and a high number-average molar mass of $26,850 \text{ g mol}^{-1}$. In addition, the prepared catalyst is easy to separate from the product and still has high efficiency after recycling. Subsequently, the author improved MOF-901 by introducing a longer linker, 4,4'-biphenyl dicarbaldehyde containing two benzene rings, as the connecting units to build MOF-902. The presence of the highly conjugated backbone promotes the red shift of visible light absorption. The new MOF-902 has better photocatalytic efficiency than MOF-901 for the polymerization of methyl methacrylate.

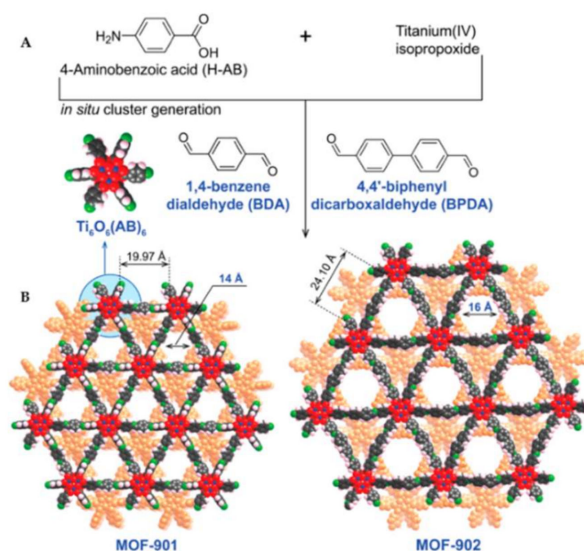


Figure 5. Synthetic procedure (A) and the structures (B) of MOF-901 and MOF-902 [71]. Copyright 2016, American Chemical Society.

2.2.2. Copper-Based MOF Catalysts

In 2016, Schmidt and his colleagues [72] presented a novel approach for atom transfer radical polymerization by designing a $\text{Cu}(\text{II})$ -based MOF named $\text{Cu}_2(\text{bdc})_2(\text{dabc})$. The $\text{Cu}(\text{II})$ centers in the MOF was reduced by amino compound to generate $\text{Cu}(\text{I})$ species as the activator for atom transfer radical polymerization of various monomers, such as benzyl methacrylate, styrene, poly(4-vinylpyridine),

and isoprene (Figure 6). Compared with the traditional catalysts that is simply made of copper halides, the Cu(II)-based MOF act as both the catalyst and the supporting ligand. Therefore, the complicated synthetic process is greatly simplified by limiting side reactions between mixture of monomers, ligands, and catalysts. In addition, considering the particle size of MOF catalyst is around several hundred nanometers, it can be easily separated from the system by centrifugation and used in other polymerization reactions. Subsequently, the research group use the Cu(II)-based MOF to catalyze the controlled radical polymerization of four nucleophilic monomers (4-vinylpyridine, 2-vinylpyridine, 2-(dimethylamino)ethyl methacrylate and methyl methacrylate) under visible light [73]. Nitrogen-containing monomers have a synergistic effect on polymerization by acting as reducing agents under irradiation. Importantly, the molecular weight of the product can be adjusted by changing the reaction time.

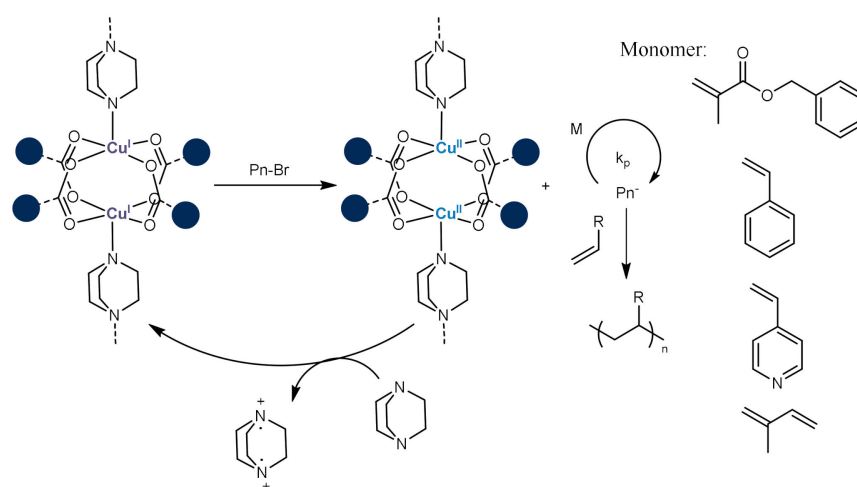


Figure 6. The structures of Cu-based MOF and the mechanism for ARGET ATRP.

Miller et al. [74] used copper-exchanged zeolite, which can mediate oxidative polymerization in air or ultrapure nitrogen (Figure 7). Inspired by the zeolite system, Marshall and his co-workers used MOF to catalyze the oxidative polymerization of thiophene monomers without adding any external oxidant. The reaction is carried out in two steps. First, oligothiophene monomers including terthiophene, poly(3,4-ethylenedioxythiophene) and 2,2'-bithiophene are filled into the pores of copper-based MOF (HKUST-1), presumably through hydrophobic interactions and coordination between thiophene group with copper. Second, oxidants are added into the system to generate polymerization in MOF. The afforded new types of nanomaterial structures may have potential applications as organic electronics. This simple and convenient oxidation protocol has inspired subsequent researchers to consider novel methods to generate MOF-guest molecules hybrid materials.

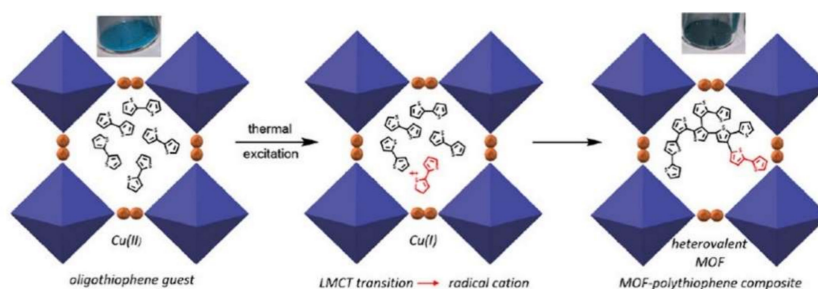


Figure 7. Schematic illustration of the host-guest composites of polythiophenes in HKUST-1 by the direct reaction of adsorbed aryl monomers [74]. Copyright 2019, American Chemical Society.

2.2.3. MOFs as Photo-Initiators for Radical Polymerization

Su group [75] studied the visible light-induced living radical polymerization using the Zr-based MOF, NNU-28 as photosensitizer (Figure 8A). These studies have shown that anthracene-based NNU-28 can function as an effective photosensitizer in the photopolymerization of methacrylate by reducing the Cu(II) complex to the activator Cu(I) complex in situ. The ATRP reaction mediated by NNU-28 proceeds under controllable conditions, which conforms to typical controllable characteristics of free radical polymerization. The prepared polymer has uniform polydispersity and good retention of chain-end activities. The visible light-initiated polymerization studied in this paper shows that photoactive polymers have broad application prospects in designed polymer synthesis.

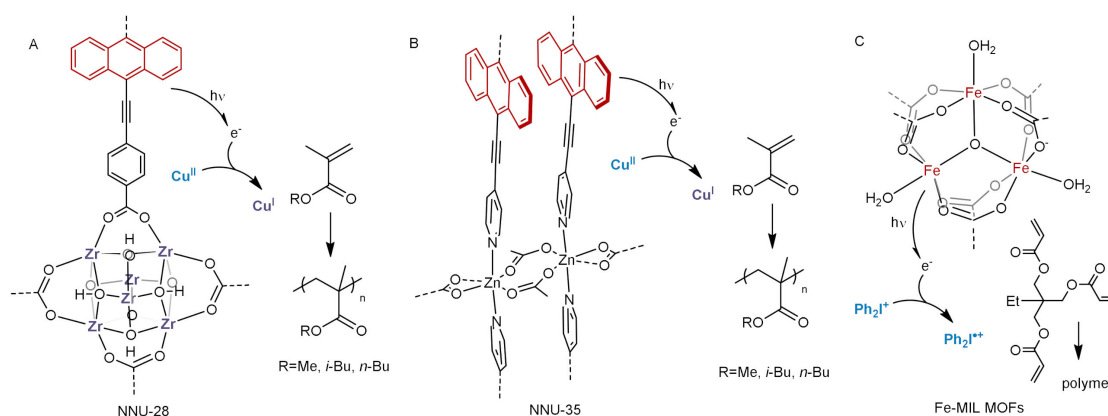


Figure 8. Scheme illustration of the mechanisms for MOF photo-initiated radical polymerization with NNU-28 (A), NNU-35 (B), and Fe-MIL MOFs (C).

Xing group [76] has developed a MOF made from photoactive anthracene-derived bipyridine, which can catalyze polymerization under visible light (Figure 8B). Subsequently, the prepared NNU-35 MOF was studied using multiple technique, such as electron paramagnetic resonance, steady state fluorescence, and single crystal X-ray diffraction. It has been shown that visible light induces the formation of free radicals in MOF structure. So, the photocatalytic ATRP of methyl acrylate monomer was realized by using MOF material as photosensitizer and the photo-reduced copper as the radical initiator. The properties of polymerization products are consistent with those of radical polymerization, including low polydispersity and high retention of chain-end activities. Therefore, the immobilization of photoactive organic ligands is an achievable method to prepare new MOF photocatalyst.

The Lalevée group [77] developed a photoinitiated system composed of highly porous Fe (III)-based MOFs, iodonium salt, and N-vinyl carbazole (Figure 8C). The acrylate in the laminate can undergo free radical polymerization driven by near UV (385 nm) or visible (405 nm) light. Under irradiation, the MOF can initiate the free-radical polymerization of trimethylolpropane triacrylate when combined with diphenyliodonium hexafluorophosphate and N-vinylcarbazole. When exposed to the air, it will promote the cationic polymerization of the epoxides. The flexible microporous Fe (III) terephthalate MIL53 stands out among the five MOFs, all of which have different chemical compositions and framework topology. The final ring-opening polymerization conversion rate of the epoxide is 58%. By introducing the MOF structure in situ during the photopolymerization process, polymer composites with strong mechanical properties can be designed.

Qiao et al. [78] used glycine-modified MOF to mimic enzyme catalysts and react with hydrogen peroxide to obtain hydroxyl groups as initiators for RAFT. Compared with natural enzyme catalysts, the MIL-53(Fe) composite still has stability and catalytic activity at high temperatures (50 °C), besides, it is non-toxic and easy to separate. The catalyzed polyacrylamides have ultra-high molecular weight ($M_n > 1$ MDa) and low dispersion ($PDI < 1.25$). This research could inspire the future use of MOFs to

mimic natural enzyme catalysis. Subsequently, combined with the previous work, their research group reported Fenton-RAFT polymerization catalyzed by Fe(II)-MOF [79] (Figure 9).

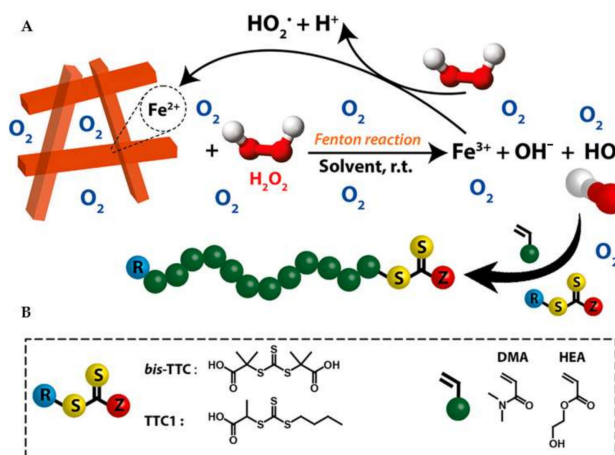


Figure 9. (A) The mechanism for Fenton-RAFT polymerization initiated by hydroxyl radicals; (B) Chemical structures of the employed trithiocarbonates (TTCs) and monomers. Copyright 2018, Royal Society of Chemistry [78].

2.3. Cationic Polymerization with Acidic MOFs

According to previous reports, solid acid catalysts have been extensively used in industry, but it is still difficult to verify the structure of Brønsted acid sites at the molecular level [80]. Yaghi et al. [81] used a series of spectroscopy, crystallography, and computational methods to explore the source of its acidity. It is finally determined that the structure of the strong Brønsted acid site in MOF-808-SO₄ is a hydrogen bond pair of water and chelated sulfate, which is composed of a specific arrangement of the water and sulfate adsorbed parts on the zirconium cluster. Acidic protons are produced by hydrogen bonding interactions. MOF-808-SO₄ enabled the dimerization of isobutylene to isoctene with high activity and selectivity, even with 100% selectivity for the C₈ products. Furthermore, the reaction was carried out for 15 days at 80 °C with no decreasing activity or selectivity of the catalyst. After the material is dehydrated, it will lose acidity and reduce the catalytic activity which verifies the importance of water for the strong acidity of the material. Therefore, when the catalyst is deactivated, it is only necessary to replenish water molecules through solvent exchange and activation near the sulfate to regenerate it.

Soon afterwards, Liu and Somorjai et al. [82] reported the use of S-MOF-808 to catalyze the polymerization of light olefins (C₃-C₆) at mild temperature and pressure (Figure 10). Although the structure of olefin is similar, different polymerization products obtained from various olefins, such as dimers, isomers, and heavier oligomers. If the second carbon atom in the main carbon chain of the olefin has an α -double bond and two substituents, then oligomerization will occur easily. In addition, it is found that there is an effective carbon-carbon coupling between isobutylene and isoamylenes, which promotes the formation of carbon-carbon bonds. In order to verify that the reaction is via a carbocation-mediated mechanism, unsaturated (vinyl) ethers were also used as substrates because alkoxy groups can improve the stability of carbocations. Subsequent studies on the deactivation and regeneration of the catalyst were carried out. The catalyst can be completely regenerated by steam treatment, which is consistent with the previous report by Yaghi group [81]. This work is an important progress for MOF-catalyzed olefin polymerization through carbocation mechanism.

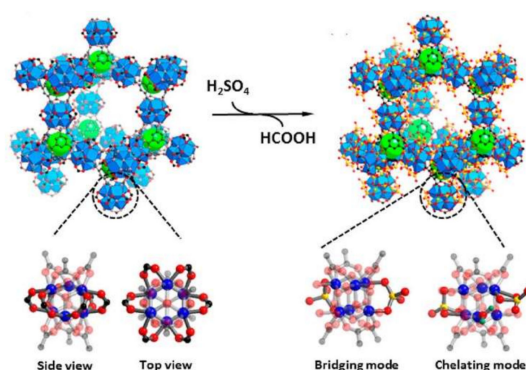
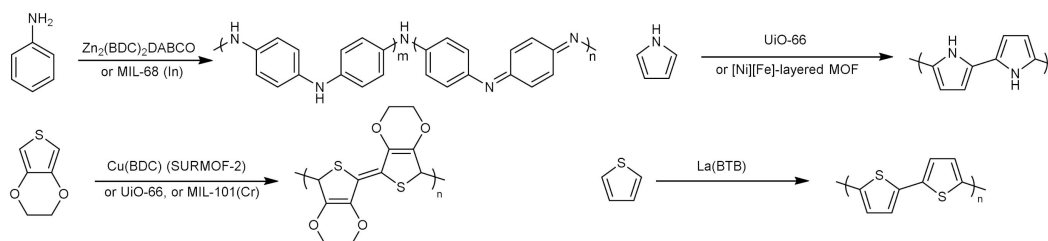


Figure 10. Structure of pristine MOF-808, sulfated S-MOF-808 [82]. Copyright 2019, American Chemical Society.

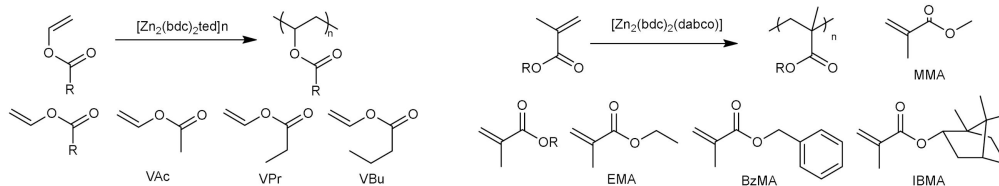
3. MOF-Templated Polymerization

As a common feature of porous materials, MOFs contain uniform cavities in the dimension of nanometers, which could be used as templates for polymerizations. In many reports, MOF-templated polymerization was achieved through covalent modifications of the SBU, or through the introduction of catalytic species. The templating effect of MOF cavity was shown to modulate the chemical and physical properties of polymerization product. This is a unique feature for catalysis in confined space, that cannot be achieved using molecular systems. The size of pores can be controlled through rational design of MOF host to obtain polymer with desirable morphology and branching, even in some cases, sequence specificity. In the following context, we will introduce the use of MOF as templates to regulate the polymerization through three categories of mechanisms (Figure 11).

Redox Polymerization



Radical Polymerization



Other Polymerizations

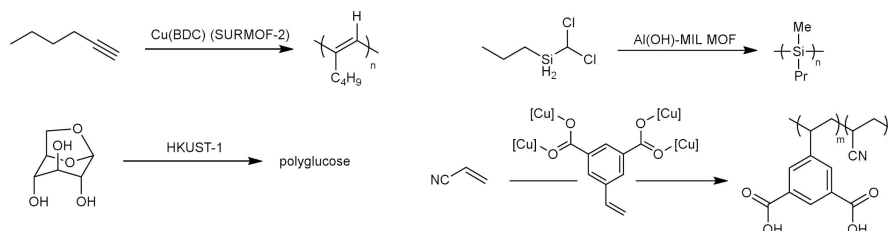


Figure 11. Summary of the polymerization reactions templated by MOFs. The types of the polymerization reactions are classified by the reaction mechanism.

3.1. MOF-Templated Polymerization with Morphology Control

3.1.1. MOF-Templated Electrochemical Polymerization

Based on previous reports, two-dimensional (2D) porous polymers with conjugated organic ligands are conductive, which include lamella covalent organic frameworks, electroactive organic frameworks [83], and conjugated microporous polymers. Although these conductive polymers have good redox properties, the low conductivity caused by the inefficient accumulation or low charge density of the p-system limits its application. Ben and Qiu et al. [84] first reported the use of MOF as a template to catalyze the synthesis of polyaniline under electrochemical conditions. The obtained 3D microporous conductive polymers have both high porosity and conductivity. MOF thin film (HKUST-1) displays high conductive and electroactive properties (electric conductivity of 0.125 S cm^{-1}), because the imine group in polyaniline combines with the carboxyl group in the MOF can transfer electrons to the porous membrane layer.

The conductivity of polyaniline generated by the electrocatalysis of HKUST-1 film cannot be measured in situ. In order to solve this problem, Klyatskaya et al. [85] added 1-hexyne monomer to the Cu-based MOF and performed potentiostatic polymerization in the 1D channel (Figure 12). The film was deposited on the prepatterned substrate through a layer-by-layer process and was detected in situ, without the need to separate the conductive polymer. The combination of the MOF with the conductive component improves the electrical conductivity of the composite material, which is increased by 8 orders of magnitude. Analysis using mass spectrometry verified that polyacetylene oligomers were formed by electropolymerization in MOFs.

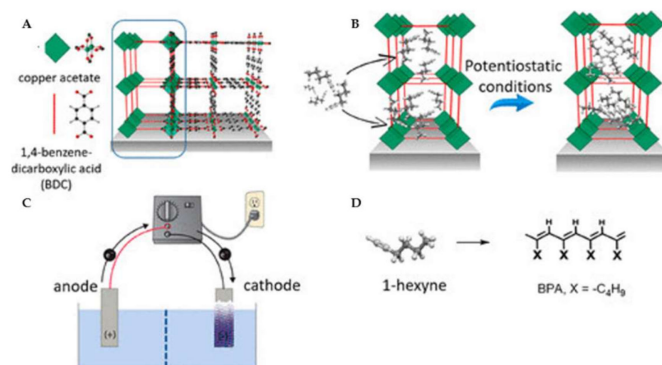


Figure 12. (A) Schematic showing the Cu(BDC) crystal structure grown along the [001] direction on a MHDA SAM. (B) Schematic showing the polymerization inside the nanochannels of SURMOF-2. (C) The setup of electrochemical cell. (D) Scheme showing the polymerization reaction of monosubstituted alkyne (1 hexyne, C₆H₁₀) [85]. Copyright 2020, American Chemical Society.

Ballav et al. [86] successfully synthesized semiconducting nanocomposites by loading conductive polypyrrole (PPy) and poly 3,4-ethylenedioxythiophene (PEDOT) chains in the cavities of a porous zirconium-based MOF (UiO-66). This strategy led to significantly higher electrical conductivity and lower thermal conductivity. PPy and PEDOT were confirmed to exist in UiO-66-PPy and UiO-66-PEDOT nanocomposites respectively by Raman and FTIR. According to PXRD and HRTEM detection, successful retention of the MOF structure and incorporation of the polymer fibers to the interstices of the frame were shown separately. The protocol provided a novel way for the synthesis of semiconducting nanocomposites with ultra-low thermal conductivity.

3.1.2. MOF-Templated Polymerizations through Redox Mechanism

The intercalative polymerization of pyrrole (Py) through oxidative polymerization in a redox-active layered coordination polymer was reported by Kitagawa in 2008 [87]. The crystallinity and morphology of the coordination polymer was retained after templating the polymerization reaction.

They manufactured oriented polymer microplates by taking advantage of the two-dimensional restriction of polymer chains in nanocomposites. The strategy will stimulate the development of 2D MOF with open structures for application in templated synthesis as reaction vessels and templates. MOF-templates thus provided a new way for redox polymerization to synthesize polypyrrole with unique morphology.

MOFs were generally known to be non-conductive. In 2016 Uemura and Kitagawa' groups [88] reported a PCP/PEDOT conductive composite with relatively high porosity. PEDOT was synthesized by oxidative polymerization of DOT in the pores of a three-dimensional MOF MIL-101(Cr) and contributed to the conductivity of the composite. The conductivity of the material could be modulated by changing the amount of the monomer added or the porosity of the MOF. Importantly, PEDOT could be used as a selective detector for NO_2 in the air. Introducing PEDOT into MOFs improved their function for gas detection with higher sensitivity.

Polythiophenes without substitution groups possess long-range conjugation, therefore exhibit unique optical and electrical properties. However, inevitable interchain interactions make them difficult to dissolve or melt. To overcome this problem, Uemura and Kitagawa group [89] adopted MOF $[\text{La}(\text{BTB})]_n$ to control the polymer assemblies (Figure 13A) by performing oxidative polymerization in the regular 1D channel of the MOF. They unprecedentedly controlled the number of polymer chains. Moreover, varying the number of polythiophene chains would alter the optical and electronic properties of the materials. Compared to the polythiophene prepared by solution polymerization, the anisotropic polymer particles has higher conductivity owing to the extended conjugate system [90]. The arrangement of macromolecules could amplify the properties of polymer materials. This method was promising to be applied to many other non-processable polymers to obtain potentially useful but not yet explored properties (Figure 13B).

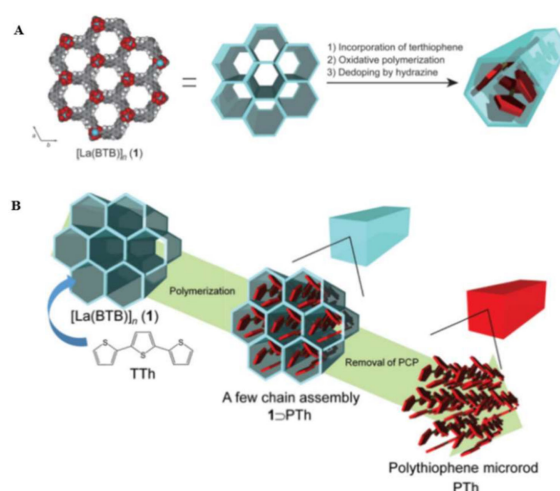


Figure 13. (A) Scheme showing the unsubstituted polythiophene inside the 1D nanochannels of $\text{La}(\text{BTB})$. (B) Scheme showing the polymerization inside the nanochannels of MOF [89,90]. Copyright 2019 by John Wiley & Sons, Inc. and 2017, Royal Society of Chemistry.

3.1.3. MOF-Templated Radical Polymerization and Click Polymerization

Subsequently, Schmidt group [91] proposed a new method for polymer synthesis through the combination of the porous MOF structures with reversible deactivation radical polymerization techniques, such as the connection of activator regenerated by electron transfer atom transfer radical polymerization to MOF. The narrow nanochannel of $\text{Zn}_2(\text{benzene-1,4-dicarboxylate})_2(1,4\text{-diazabicyclo}[2.2.2]\text{-octane})$ is used as the template for the polymerization of various methacrylate monomers (benzyl, methyl, ethyl, and isobornyl methacrylate), resulting in the polymer being able to adjust the dispersion, function and viscosity of different molecular sizes (Figure 14). In order to further improve

and strengthen the influence of the initiator functionalized ligand on the polymer, by combining the initiator functionalized ligand Brbdc co-crystallized. The initiator-functionalized MOF was synthesized in various proportions (10%, 20%, and 50%). The ARGET ATRP is directly activated from the wall of the nanochannel via the embedded initiator. The molecular weight of the obtained polymer is as high as 392,000. In addition, significant improvements in terminal function and steric control were observed, giving the polymer a significant increase in isotacticity. This result highlights the combination of MOF and ATRP, which is a significant potential and versatile method with significant potential for the production of various polymers with high molecular weight. These polymers have superior performance in chain length, microstructure and retention of chains.

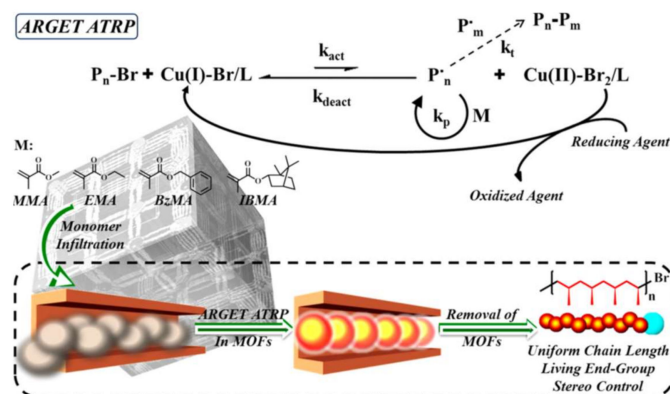


Figure 14. Scheme showing the ARGET ATRP in the nanochannel of MOF for the synthesis of well-defined polymers [91]. Copyright 2018, American Chemical Society.

Schmid et al. [92] reported in 2017 that MOF $[\text{Zn}_2(\text{bdc})_2\text{ted}]_n$ was used as a template for reversible deactivation radical polymerization (RDRP) and reversible addition-fragmentation chain transfer polymerization in its nanochannels. By using different molecular sizes of vinyl ester which is vinyl acetate, vinyl propionate and vinyl butyrate, the effect of size on radical polymerization was investigated. The results showed that as the monomer size increased, the conversion rate, molecular weight, and crystallization decreased. This is the first time that MOF has been applied to the RDRP field.

In 2020, Xing et al., synthesized two zirconium-porphyrin MOFs with *csq* topology, using Zr_6 -clusters as the SBU and porphyrin tetracarboxylate ligands (H_2TCPP or Zn-TCPP) as the photosensitive units. Irradiation of visible light induces charge separation and migration, thus the zirconium-porphyrin MOF can activate Cu(II) to initiate the polymerization of methacrylate through a single electron transfer process. The prepared polymer has a uniform distribution of molecular weight and high retention of chain-end groups [93].

Kokado and Sada et al. [94] reported that two different monomers were copolymerized step by step assisted by the templating effect of MOFs. First, the crystalline A monomer is fixed in the ZnAz MOF frame, the B monomer can enter through the pores of the MOF in the solution and copolymerized to form a linear polymer. After the ZnAzMOF is eliminated in CL2 (Figure 15), the obtained polymer has the same unit structure as the polymer produced by solution polymerization, but is not significantly affected by the consumption of monomer reaction site and apparent stoichiometry of the monomer. Moreover, polymer with different degrees of polymerization is affected by the arrangement of the monomers in the ZnAzMOF , which opens up a new way to design a predictable degree of polymerization by changing the arrangement of the monomers.

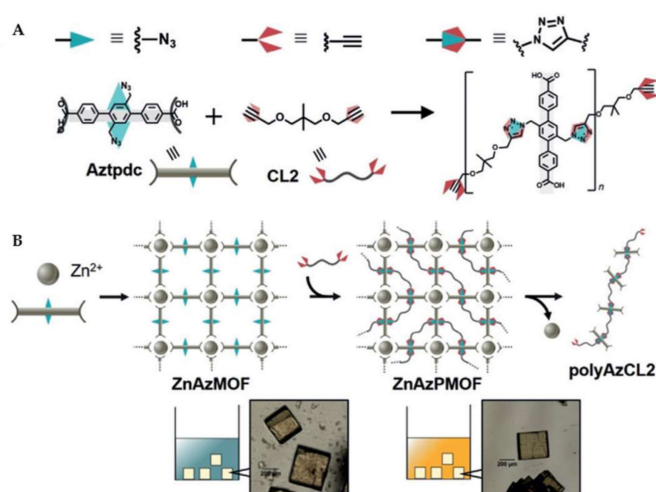


Figure 15. (A) Scheme showing the polymerization of Aztpdc and CL2 by the azide–alkyne click reaction. (B) Scheme showing the polymerization of Aztpdc and CL2 in ZnAzMOF to obtain linear polymer. The appearance of ZnAzMOF (left) and ZnAzPMOF (right) by optical microscopy images [94]. Copyright 2019 by John Wiley & Sons, Inc.

3.1.4. MOF-Templated Polycondensation

Yuichiro Kobayashi et al. [95] synthesized the polysaccharide within the three-dimensional nanochannel of HKUST-1 and effectively controlled the porosity and particle size of the polysaccharide (Figure 16). The resulting material has larger specific surface area and higher loading capacity for drug molecules and proteins. Polysaccharides obtained by the MOF-templated polymerization is not only effective in drug release, but also effective in adsorption and filtration, and can be used as an immobilized carrier.

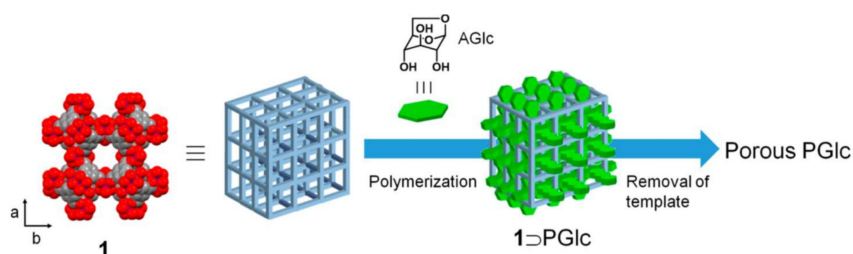


Figure 16. Scheme showing the polymerization of porous polyglucose using MOF HKUST-1 as the host matrix. View of three-dimensional nanochannels of HKUST-1 displayed using a space-filling model (O, red; C, gray; Cu, blue) [95]. Copyright 2017, American Chemical Society.

Polysilanes are a kind of polymer that exhibit unique optical and electrical properties. Due to the delocalization of σ -electron, polysilanes possess high mobility of charge carriers and high fluorescence quantum yield, which is influenced by the conformation of the main chain to a large extent. Besides, Si-Si bond is easy to cleave under UV irradiation to produce silyl and silylenes, which lead to the formation of less conjugate structure. By directly encapsulating polymethylpropylsilane into the nanochannels of a series of aluminum MOFs, Uemura and Kitagawa group [96] successfully isolated single polysilanes chains which is difficult to achieve using conventional methods. Importantly, the conformation of the isolated chains could be controlled by varying the channel environment of the MOFs, thereby generating polysilanes with better carrier mobility than the bulk material. In addition, photodegradation of the polymers under UV could be avoided. The nanochannels keep the intermediates formed through the cleavage of Si-Si bond away from oxygen and stabilize the intermediates for recombination.

3.2. MOF-Templated Sequence-Specific and Crosslinking-Specific Polymerization

The polymers obtained through solution chemistry has the locked conformations and physical entanglements owing to the different vinyl monomers copolymerization in a topologically disordered fashion. In 2013, the Kitagawa group [97] reported a reactive scaffold to reveal the reactive portion of the inner surface of the micropores and to create crosslinking sites between specific polymer chains. In this way, the newly synthesized polymer materials show unconventional properties. Host–guest cross polymerization has thus been studied as a new way for the synthesis of crosslinked polymers with pseudo crystallinity. First, the crosslink keeps the main chain at a defined distance in the register and is fully integrated into the pseudo crystalline state. Secondly, pseudo-crystallinity is an amorphous polymer chain which is not resistant to crystallization when it exists. Third, polymer chains are permanently aligned in parallel by bundling adjacent chains together. Finally, the precise sequence of MOF hosts is transferred to polymer materials at both molecular and morphological levels. In addition, the retainment of crystallinity and its stability at high temperatures offer the potential of improving the mechanical and thermal properties of polymer materials. Therefore, this strategy can be widely applied to polymerize vinyl monomers in MOFs that provide suitable ligands, resulting in a series of polymer materials endowed with functional properties and highly anisotropic structures.

It is a challenging research subject to design the sequence of monomers in polymers. In this field, the free-radical polymerization to obtain the vinyl copolymers faced severe challenges. In 2018, Uemura group [98] reported the strategy to utilize the periodic structure of MOF as a template to generate the sequence-regulated vinyl copolymers. Mixing of styrene-3,5-dicarboxylic acid (S) and Cu^{2+} leads to a $[\text{Cu}(\text{styrene-3,5-dicarboxylate})]_n$, in which the styryl groups immobilized periodically along the one-dimensional channels (Figure 17). After the hole of MOF was introduced the acrylonitrile (A), inside the channel happening the radical copolymerization between the immobilized S and A. Following, the MOF is decomposed to isolate the copolymer. The monomer composition, theoretical calculations and NMR spectroscopy conformed the predominantly repetitive SAAA sequence. The copolymerization of methyl vinyl ketone also provided the same type of sequence-regulated copolymer, suggesting that the method has the capability to control copolymer sequences at the molecular level by transcriptional MOF cycles.

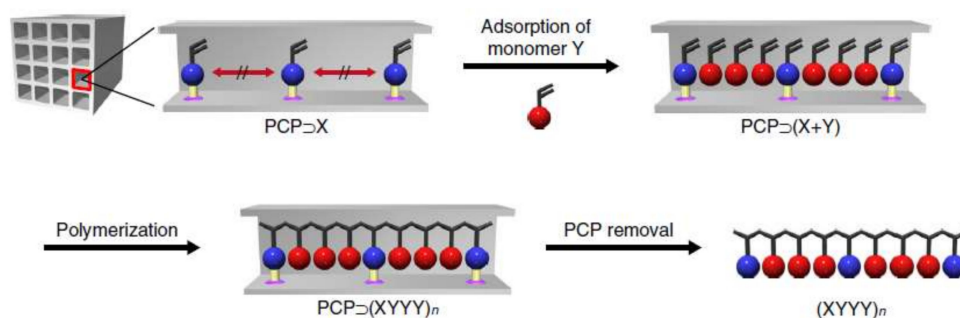


Figure 17. Scheme showing the sequence-regulated radical copolymerization using MOFs $[\text{Cu}(\text{styrene-3,5-dicarboxylate})]_n$ [98]. Copyright 2018, Nature Publishing Group.

3.3. MOF-Templated Regioselective and Branching-Selective Polymerization

The specific interaction sites on and in nanochannels, Therefore, functionalized MOFs have been regarded with useful catalytic applications in polymer and organic synthesis. For the advantage of being able to accelerate reactions, regulate and control reactions (stereoscopic and regional control), and substrate specificity, which are analogous to enzyme reactions in biosystem. In 2006, Kitagawa and collaborators [99] reported the truly designable MOFs $[\text{Cu}_2(\text{pzdc})_2(\text{L})]_n$ providing specific basic interaction sites in nanochannels, accelerating the stereoscopic control and monoselective polymerization of substituted acetylene. This strategy will promote the development of hybrid MOF materials. On the other hand, a novel host/guest nanostructure for fundamental study and applications

of these polymers possessing MOF filled with π -conjugate. Subsequently, his group [100] continue designed nanochannels of MOF with different pore sizes and applied them to topotactic selective radical polymerization of divinylbenzenes (Figure 18). Studies have shown that large channels would cause branching, while small channels would cause limited adsorption of monomer, only the proper channel size can polymerize selectively olefins.

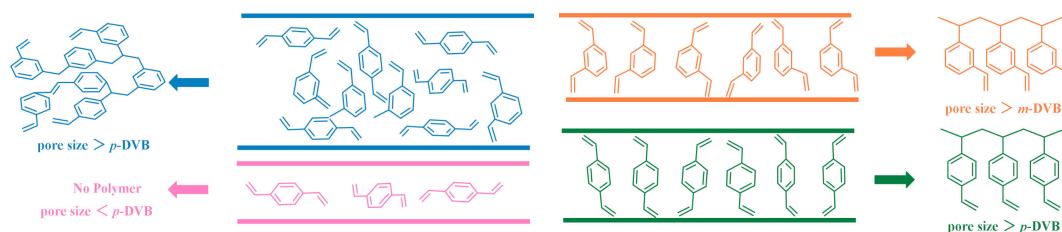


Figure 18. Mechanism of the nanochannel-affected polymerization in MOFs $[\text{Cu}_2(\text{pzdc})_2(\text{L})]_n$.

Uemura et al. [101] successfully prepared a series of MOFs $[\text{Cu}_2(\text{L})_2(\text{ted})]_n$ by introducing different kinds of substituents to the organic ligand L (L = dicarboxylates ligands) to regulate the radical polymerization of MMA. The most favorable characteristics of MOF was the ability of surface functionalization through different substituents. The number and location of substituent groups strongly affected the tacticity of the PMMA. Moreover, the authors observed the remarkable effect of substituents on the stereoregularity of PMMA via experimental and theoretical analysis, mainly including N_2 adsorption, IR, a statics study, and molecular dynamics calculations. It is worth noting that tacticity of PMMA greatly changed owing to the specific channel shape of 2OMe (narrow, regular, and helically twisted channels).

In the free radical polymerization of vinyl monomers with two functional groups, regardless of bulk polymerization or solution polymerization, it is difficult to avoid cross-linking reactions to obtain insoluble polymers. The current solution to this problem is to reduce the product of monofunctional polymerization, which is designed according to the structure of the monomer. But it follows that this method, non-conjugated structure leads to a low degree of polymerization. Uemura et al. [102] used the narrow nanochannels in the MOF as a template polymerize 1,6-diene to form a soluble linear polymer, which can inhibit side reactions such as chain transfer and chain termination (Figure 19A). Furthermore, the pore structure of MOFs can be functionalized by different kinds of organic ligands to control the morphology of polymers. Subsequently, the Uemura and Kitagawa group [103] used MOF for the polymerization of glucose. By the same mechanism, the nanochannel of MOF effectively limits the side reaction of branching to obtain quasi-linear polyglucose (PGlc) (Figure 19B).

As mentioned above, the metal at the inorganic site affects the selectivity of olefin polymerization. Weckhuysen et al. [104] proposed that the linker and pore structure also play a key role. They used MIL-100 and MIL-101 MOFs with the same metal and topological structure to polymerize olefins, but only the latter has catalytic activity. Scanning electron microscopy studies showed that the structure of MIL101 completely collapsed after adding organoaluminum co-catalyst which cleaves Cr–O bonds to generate alkylated Cr species. These species are responsible for catalyzing the formation of amorphous polyethylene beads. XRD research shows that MIL-100 is still crystalline after adding organoaluminum catalyst and has high stability against fragmentation, so it does not have the activity of catalyzing olefins. In-situ infrared spectroscopy and ultraviolet-visible-near-infrared spectroscopy showed that different metal oxides form different reduction and alkylation chromium sites on inorganic sites, which shows the importance of linkers in synthesis catalysts. They found a new influencing factor on the selectivity and activity of MOFs to catalyze olefin polymerization, which is conducive to the synthesis of MOFs with high performance.

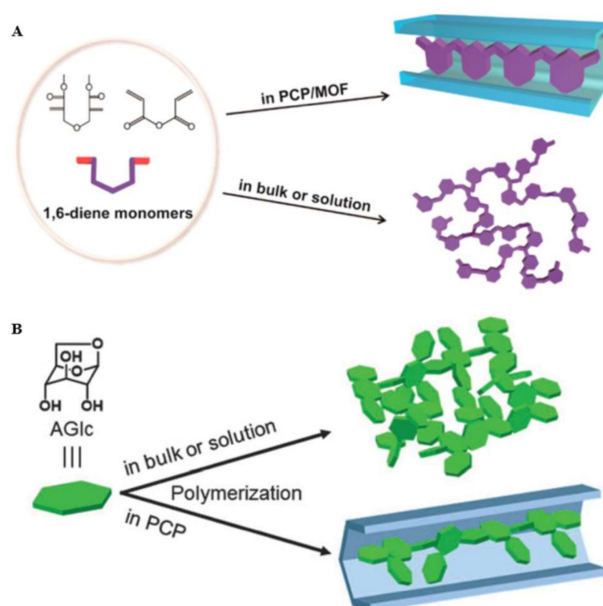


Figure 19. (A) Scheme showing the polymerization of 1,6-diene in MOF channel and in bulk or solution. (B) Polymerization of AGlc in bulk, solution, and 1D nanochannels of MOFs [102,103]. Copyright 2014, American Chemical Society.

4. Overview and Outlook

In this review, we summarized the application of MOF for oligomerization and polymerization reactions into two categories. The first category summarizes the use of various MOFs with catalytically active reaction sites to catalyze polymerization, the other is the use of MOFs to provide confined space with specific sizes and shapes to control polymerization. First, MOF catalyze polymerization and oligomerization mainly through three types mechanisms, including organometallic, radical and cationic mechanisms. For polymerization through organometallic mechanism, we organized the section into MOF catalysts with different types of metal active sites, including Zr, Ni, Co, V, Cr, and Ln. In addition, MOF can initiate radical polymerization as photocatalyst, photo-initiator, or host of photocatalysts. For cationic polymerization, acidic or superacidic MOFs were shown to effectively catalyze polymerization reactions. The second half of our review described the use of MOFs as templates to control polymerization, over various properties including morphology, regioselectivity, and even sequence specificity. The straightforward strategy is to synthesize polymers with specific morphologies, either as 1D fibers, 2D plates, or 3D porous structures, through the templating effect of MOF channels. More interestingly, the hydrophobic confinement effect, in combination with various polar interactions between monomers and the MOF channel, polymerization could be fine-tuned to control branching, regio- and stereo-selectivity, and even in scarce examples, sequence specificity.

Moving forward, what is the next goal for MOF-catalyzed and MOF-templated polymerization? In view of all the established achievements in this field that we summarized in this review, we believe that MOF-templated polymerization with sequence specificity is the direction that is underexplored, yet with great potential applications. If we look the mechanism for the ribosomal synthesis of protein, we immediately realize that MOF-catalyzed or templated polymerization still have a long way to go toward the ultimate goal of sequence-specific polymerization. The main function of ribosomes are to translate the sequence of nucleotide into the sequence of amino acids, therefore, to construct protein polymers from 20 types of amino acid monomers. This can be related to the aforementioned synthesis of sequenced polymers through MOF catalysis. Ribosomes use large conformational changes to quickly and accurately identify suitable tRNAs and align them for the sequence-specific formation of amide bonds (Figure 20A).

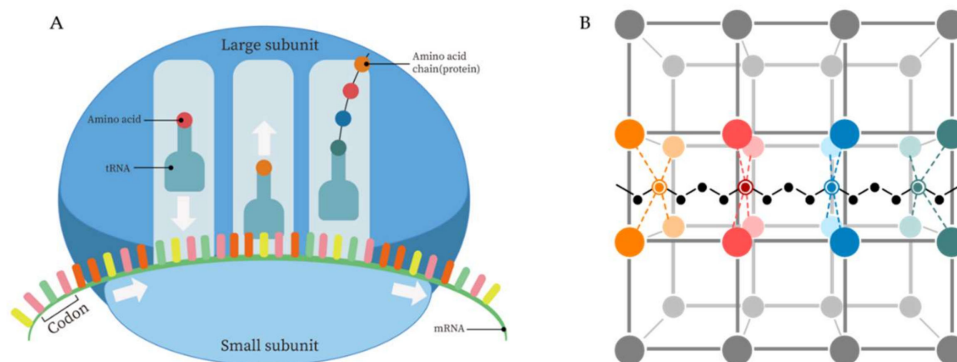


Figure 20. (A) The schematic representation of the mechanism for ribosome-catalyzed sequence-specific polymerization of amino acids. (B) An outlook of the challenging goal of MOF-templated sequence-specific polymerization using multivariate MOF.

MOF shares at least three similar features to the ribosome, which make MOF the ideal candidate for achieving sequence-specific polymerizations. Firstly, both MOF and ribosome catalyze polymerization in confined space, which allows the catalyst to take advantage of the synergistic action of various non-covalent and covalent interactions to align different monomers. The accurate and tunable nanochannel in MOF have the potential to be accurately designed to control polymerization. Secondly, with the continuous development of multivariate MOFs (MTV MOFs), [105–108] the conventional periodic structure could now incorporate structural diversity with sequential information (Figure 20B).

The design of ribosome-mimetic MOFs for sequence-specific polymerization also resonance with the ongoing research interest in the design of enzyme-mimetic MOF catalysts. The weak-field coordination environment around the metal centers in the SBU, the customizable and shape-specific pores and channels of MOFs, and the hydrophobicity of aryl linkers all indicated the similarity between MOFs and biocatalysts [109]. For example, the zinc centers in MOF SBU was studied to mimic carbonic anhydrase [110]. MOFs have also been designed as hydrogen-bonding catalysts by introducing urea and thiourea into the MOF channel, which mimics the function of arginine [111–114]. Multiple other works have reported the use of MOF catalysts mimic phosphotriesterase, cytochrome P450, hydrogenase to function as catalysts for hydrolyzing nerve agent simulants [115], transporting oxygen [116], and for generating hydrogen [117–119]. Following similar strategy of biomimicry, future research in MOF-catalyzed and MOF-templated polymerization could design and synthesize ribosome-mimetic MOFs. This goal is still a fantasy but could be realized with continuous and collaborative efforts toward the development of multivariate MOFs with built-in sequential information. Such sequence-specific polymerization has great potential for the synthesis of advanced polymers.

Author Contributions: Writing and editing the review, F.R. and P.J.; supervision, P.J. All authors have read and agreed to the published version of the manuscript.

Funding: This research received no external funding.

Acknowledgments: P.J. acknowledges support from the Miller Institute for Basic Research in Science at the University of California, Berkeley.

Conflicts of Interest: The authors declare no conflict of interest.

Abbreviations

1D	one-dimensional
2D	two-dimensional
2,6-ndc	2,6-naphthalenedicarboxylate
3D	three-dimensional
ATRP	atom transfer radical polymerization
bdc	para-terephthalate, or 1,4-benzene dicarboxylate
BTB	1,3,5-benzotrisbenzoate
Brbdc	2-(2-bromo-2-methylpropanamido)-1,4-benzenedicarboxylate
CFA-1	Zn ₅ (OAc) ₄ (bibtz) ₃
dabco	1,4-diazabicyclo[2.2.2]octane
DOT	dioxythiophene
DNA	deoxyribonucleic acid
form	formate
H ₂ BTDD	bis(1H-1,2,3-triazolo[4,5-b],[4',5'-i])dibenzo[1,4]dioxin
MOF	Metal-organic framework
MMAO-12	methylaluminoxane-12
MFU-4l	Zn ₅ Cl ₄ (BTDD) ₃
MMA	methyl methacrylate
mRNA	messenger RNA
NMR	Nuclear Magnetic Resonance
Ni ₂ (dobdc)	dobdc = 2,5-dioxido-1,4-benzenedicarboxylate; Ni-MOF-74
Ni ₂ (dobpdc)	dobpdc = 4,4'-dioxido-[1,1'-biphenyl]-3,3'-dicarboxylate
ox	oxalate
PPy	polypyrrole
PEDOT	poly 3,4-ethylenedioxythiophene
PMMA	poly(methylmethacrylate)
PDI	polydispersity
pzdc	pyrazine-2,3-dicarboxylate
PGlc	polyglucose
RAFT	reversible addition-fragmentation chain transfer
SBU _s	secondary building units
Tp ^{Mes}	HB(3-mesitylpyrazolyl) ₃
ted	triethylenediamine
tRNA	transfer RNA
TTC _s	trithiocarbonates
UV	ultraviolet
XRD	X-ray diffraction
Zn ₂ (bdc) ₂ (dabco)	Zn ₂ (benzene-1,4-dicarboxylate) ₂ (1,4-diazabicyclo[2.2.2]-octane)
ZrMe-BTC	Zr ₆ (μ ₃ -O) ₄ (μ ₃ -OLi) ₄ Me ₆ -benzene tricarboxylates

References

1. Zhou, H.C.; Long, J.R.; Yaghi, O.M. Introduction to metal-organic frameworks. *Chem. Rev.* **2012**, *112*, 673–674. [[CrossRef](#)] [[PubMed](#)]
2. Furukawa, H.; Cordova, K.E.; O’Keeffe, M.; Yaghi, O.M. The chemistry and applications of metal-organic frameworks. *Science* **2013**, *341*, 1230444. [[CrossRef](#)] [[PubMed](#)]
3. Cook, T.R.; Zheng, Y.R.; Stang, P.J. Metal-organic frameworks and self-assembled supramolecular coordination complexes: Comparing and contrasting the design, synthesis, and functionality of metal-organic materials. *Chem. Rev.* **2013**, *113*, 734–777. [[CrossRef](#)] [[PubMed](#)]
4. Cohen, S.M. Postsynthetic methods for the functionalization of metal-organic frameworks. *Chem. Rev.* **2012**, *112*, 970–1000. [[CrossRef](#)] [[PubMed](#)]
5. Rocha, J.; Carlos, L.D.; Paz, F.A.; Ananias, D. Luminescent multifunctional lanthanides-based metal-organic frameworks. *Chem. Soc. Rev.* **2011**, *40*, 926–940. [[CrossRef](#)]

6. Zhao, X.; Wang, Y.; Li, D.S.; Bu, X.; Feng, P. Metal-Organic Frameworks for Separation. *Adv. Mater.* **2018**, *30*, 1705189. [[CrossRef](#)]
7. Li, J.R.; Sculley, J.; Zhou, H.C. Metal-organic frameworks for separations. *Chem. Rev.* **2012**, *112*, 869–932. [[CrossRef](#)]
8. Li, J.-R.; Ma, Y.; McCarthy, M.C.; Sculley, J.; Yu, J.; Jeong, H.-K.; Balbuena, P.B.; Zhou, H.-C. Carbon dioxide capture-related gas adsorption and separation in metal-organic frameworks. *Coord. Chem. Rev.* **2011**, *255*, 1791–1823. [[CrossRef](#)]
9. Zhang, Y.; Yuan, S.; Day, G.; Wang, X.; Yang, X.; Zhou, H.-C. Luminescent sensors based on metal-organic frameworks. *Coord. Chem. Rev.* **2018**, *354*, 28–45. [[CrossRef](#)]
10. Kreno, L.E.; Leong, K.; Farha, O.K.; Allendorf, M.; Van Duyne, R.P.; Hupp, J.T. Metal-organic framework materials as chemical sensors. *Chem. Rev.* **2012**, *112*, 1105–1125. [[CrossRef](#)]
11. Hu, Z.; Deibert, B.J.; Li, J. Luminescent metal-organic frameworks for chemical sensing and explosive detection. *Chem. Soc. Rev.* **2014**, *43*, 5815–5840. [[CrossRef](#)] [[PubMed](#)]
12. Burtch, N.C.; Heinen, J.; Bennett, T.D.; Dubbeldam, D.; Allendorf, M.D. Mechanical Properties in Metal-Organic Frameworks: Emerging Opportunities and Challenges for Device Functionality and Technological Applications. *Adv. Mater.* **2018**, *30*, 1704124. [[CrossRef](#)] [[PubMed](#)]
13. Horcajada, P.; Gref, R.; Baati, T.; Allan, P.K.; Maurin, G.; Couvreur, P.; Ferey, G.; Morris, R.E.; Serre, C. Metal-organic frameworks in biomedicine. *Chem. Rev.* **2012**, *112*, 1232–1268. [[CrossRef](#)] [[PubMed](#)]
14. Horcajada, P.; Chalati, T.; Serre, C.; Gillet, B.; Sebrie, C.; Baati, T.; Eubank, J.F.; Heurtaux, D.; Clayette, P.; Kreuz, C.; et al. Porous metal-organic-framework nanoscale carriers as a potential platform for drug delivery and imaging. *Nat. Mater.* **2010**, *9*, 172–178. [[CrossRef](#)]
15. Sumida, K.; Rogow, D.L.; Mason, J.A.; McDonald, T.M.; Bloch, E.D.; Herm, Z.R.; Bae, T.H.; Long, J.R. Carbon dioxide capture in metal-organic frameworks. *Chem. Rev.* **2012**, *112*, 724–781. [[CrossRef](#)]
16. Suh, M.P.; Park, H.J.; Prasad, T.K.; Lim, D.W. Hydrogen storage in metal-organic frameworks. *Chem. Rev.* **2012**, *112*, 782–835. [[CrossRef](#)]
17. D’Alessandro, D.M.; Smit, B.; Long, J.R. Carbon dioxide capture: Prospects for new materials. *Angew. Chem. Int. Ed. Engl.* **2010**, *49*, 6058–6082. [[CrossRef](#)]
18. Jiao, L.; Wang, Y.; Jiang, H.L.; Xu, Q. Metal-Organic Frameworks as Platforms for Catalytic Applications. *Adv. Mater.* **2018**, *30*, 1703663. [[CrossRef](#)]
19. Lee, J.; Farha, O.K.; Roberts, J.; Scheidt, K.A.; Nguyen, S.T.; Hupp, J.T. Metal-organic framework materials as catalysts. *Chem. Soc. Rev.* **2009**, *38*, 1450–1459. [[CrossRef](#)]
20. Ma, L.; Abney, C.; Lin, W. Enantioselective catalysis with homochiral metal-organic frameworks. *Chem. Soc. Rev.* **2009**, *38*, 1248–1256. [[CrossRef](#)]
21. Kitagawa, S.; Kitaura, R.; Noro, S. Functional porous coordination polymers. *Angew. Chem. Int. Ed. Engl.* **2004**, *43*, 2334–2375. [[CrossRef](#)] [[PubMed](#)]
22. Cavka, J.H.; Jakobsen, S.; Olsbye, U.; Guillou, N.; Lamberti, C.; Bordiga, S.; Lillerud, K.P. A New Zirconium Inorganic Building Brick Forming Metal Organic. *J. Am. Chem. Soc.* **2008**, *130*, 13850–13851. [[CrossRef](#)] [[PubMed](#)]
23. Hyde, S.T.; Chen, B.; O’Keeffe, M. Some equivalent two-dimensional weavings at the molecular scale in 2D and 3D metal-organic frameworks. *CrystEngComm* **2016**, *18*, 7607–7613. [[CrossRef](#)]
24. Perez-Ramirez, J.; Christensen, C.H.; Egeblad, K.; Christensen, C.H.; Groen, J.C. Hierarchical zeolites: Enhanced utilisation of microporous crystals in catalysis by advances in materials design. *Chem. Soc. Rev.* **2008**, *37*, 2530–4252. [[CrossRef](#)] [[PubMed](#)]
25. Bosch, M.; Yuan, S.; Rutledge, W.; Zhou, H.C. Stepwise Synthesis of Metal-Organic Frameworks. *Acc. Chem. Res.* **2017**, *50*, 857–865. [[CrossRef](#)] [[PubMed](#)]
26. Lu, G.; Li, S.; Guo, Z.; Farha, O.K.; Hauser, B.G.; Qi, X.; Wang, Y.; Wang, X.; Han, S.; Liu, X.; et al. Imparting functionality to a metal-organic framework material by controlled nanoparticle encapsulation. *Nat. Chem.* **2012**, *4*, 310–316. [[CrossRef](#)]
27. Farha, O.K.; Eryazici, I.; Jeong, N.C.; Hauser, B.G.; Wilmer, C.E.; Sarjeant, A.A.; Snurr, R.Q.; Nguyen, S.T.; Yazaydin, A.O.; Hupp, J.T. Metal-organic framework materials with ultrahigh surface areas: Is the sky the limit? *J. Am. Chem. Soc.* **2012**, *134*, 15016–15021. [[CrossRef](#)]
28. Ploetz, E.; Engelke, H.; Lächelt, U.; Wuttke, S. The Chemistry of Reticular Framework Nanoparticles: MOF, ZIF, and COF Materials. *Adv. Funct. Mater.* **2020**, *30*, 1909062. [[CrossRef](#)]

29. Yang, P.; Zhao, W.; Shkurenko, A.; Belmabkhout, Y.; Eddaoudi, M.; Dong, X.; Alshareef, H.N.; Khashab, N.M. Polyoxometalate-Cyclodextrin Metal-Organic Frameworks: From Tunable Structure to Customized Storage Functionality. *J. Am. Chem. Soc.* **2019**, *141*, 1847–1851. [[CrossRef](#)]
30. Stuart, M.A.; Huck, W.T.; Genzer, J.; Muller, M.; Ober, C.; Stamm, M.; Sukhorukov, G.B.; Szleifer, I.; Tsukruk, V.V.; Urban, M.; et al. Emerging applications of stimuli-responsive polymer materials. *Nat. Mater.* **2010**, *9*, 101–113. [[CrossRef](#)]
31. de Las Heras Alarcon, C.; Pennadam, S.; Alexander, C. Stimuli responsive polymers for biomedical applications. *Chem. Soc. Rev.* **2005**, *34*, 276–285. [[CrossRef](#)] [[PubMed](#)]
32. Biju, V. Chemical modifications and bioconjugate reactions of nanomaterials for sensing, imaging, drug delivery and therapy. *Chem. Soc. Rev.* **2014**, *43*, 744–764. [[CrossRef](#)] [[PubMed](#)]
33. Uemura, T.; Kitagawa, K.; Horike, S.; Kawamura, T.; Kitagawa, S.; Mizuno, M.; Endo, K. Radical polymerisation of styrene in porous coordination polymers. *Chem. Commun.* **2005**, *48*, 5968–5970. [[CrossRef](#)] [[PubMed](#)]
34. Uemura, T.; Yanai, N.; Kitagawa, S. Polymerization reactions in porous coordination polymers. *Chem. Soc. Rev.* **2009**, *38*, 1228–1236. [[CrossRef](#)]
35. Begum, S.; Hassan, Z.; Brase, S.; Tsotsalas, M. Polymerization in MOF-Confined Nanospaces: Tailored Architectures, Functions, and Applications. *Langmuir* **2020**, *36*, 10657–10673. [[CrossRef](#)]
36. Walsh, D.J.; Hyatt, M.G.; Miller, S.A.; Guironnet, D. Recent Trends in Catalytic Polymerizations. *ACS Catal.* **2019**, *9*, 11153–11188. [[CrossRef](#)]
37. D'Amore, M.; Thushara, K.S.; Piovano, A.; Causà, M.; Bordiga, S.; Groppo, E. Surface Investigation and Morphological Analysis of Structurally Disordered MgCl₂ and MgCl₂/TiCl₄ Ziegler–Natta Catalysts. *ACS Catal.* **2016**, *6*, 5786–5796. [[CrossRef](#)]
38. Credendino, R.; Liguori, D.; Fan, Z.; Morini, G.; Cavallo, L. Toward a Unified Model Explaining Heterogeneous Ziegler–Natta Catalysis. *ACS Catal.* **2015**, *5*, 5431–5435. [[CrossRef](#)]
39. Grau, E.; Lesage, A.; Norsic, S.; Copéret, C.; Monteil, V.; Sautet, P. Tetrahydrofuran in TiCl₄/THF/MgCl₂: A Non-Innocent Ligand for Supported Ziegler–Natta Polymerization Catalysts. *ACS Catal.* **2012**, *3*, 52–56. [[CrossRef](#)]
40. Astruc, D.; Lu, F.; Aranzas, J.R. Nanoparticles as recyclable catalysts: The frontier between homogeneous and heterogeneous catalysis. *Angew. Chem. Int. Ed. Engl.* **2005**, *44*, 7852–7872. [[CrossRef](#)]
41. Yoon, M.; Srirambalaji, R.; Kim, K. Homochiral metal-organic frameworks for asymmetric heterogeneous catalysis. *Chem. Rev.* **2012**, *112*, 1196–1231. [[CrossRef](#)] [[PubMed](#)]
42. Wang, Y.; Wang, X.; Antonietti, M. Polymeric graphitic carbon nitride as a heterogeneous organocatalyst: From photochemistry to multipurpose catalysis to sustainable chemistry. *Angew. Chem. Int. Ed. Engl.* **2012**, *51*, 68–89. [[CrossRef](#)] [[PubMed](#)]
43. Li, Z.X.; Zou, K.Y.; Zhang, X.; Han, T.; Yang, Y. Hierarchically Flower-like N-Doped Porous Carbon Materials Derived from an Explosive 3-Fold Interpenetrating Diamondoid Copper Metal-Organic Framework for a Supercapacitor. *Inorg. Chem.* **2016**, *55*, 6552–6562. [[CrossRef](#)]
44. Thomas, T.; Dixon, M.P.; Kueh, A.J.; Voss, A.K. Mof (MYST1 or KAT8) is essential for progression of embryonic development past the blastocyst stage and required for normal chromatin architecture. *Mol. Cell. Biol.* **2008**, *28*, 5093–5105. [[CrossRef](#)] [[PubMed](#)]
45. Fracaroli, A.M.; Siman, P.; Nagib, D.A.; Suzuki, M.; Furukawa, H.; Toste, F.D.; Yaghi, O.M. Seven Post-synthetic Covalent Reactions in Tandem Leading to Enzyme-like Complexity within Metal-Organic Framework Crystals. *J. Am. Chem. Soc.* **2016**, *138*, 8352–8355. [[CrossRef](#)] [[PubMed](#)]
46. Strobel, S.A.; Cochrane, J.C. RNA catalysis: Ribozymes, ribosomes, and riboswitches. *Curr. Opin. Chem. Biol.* **2007**, *11*, 636–643. [[CrossRef](#)]
47. Erlacher, M.D.; Polacek, N. Ribosomal catalysis: The evolution of mechanistic concepts for peptide bond formation and peptidyl-tRNA hydrolysis. *RNA Biol.* **2008**, *5*, 5–12. [[CrossRef](#)]
48. Pitzer, J.; Steiner, K. Amides in Nature and Biocatalysis. *J. Biotechnol.* **2016**, *235*, 32–46. [[CrossRef](#)]
49. Hagner, P.R.; Mazan-Mamczarz, K.; Dai, B.; Balzer, E.M.; Corl, S.; Martin, S.S.; Zhao, X.F.; Gartenhaus, R.B. Ribosomal protein S6 is highly expressed in non-Hodgkin lymphoma and associates with mRNA containing a 5' terminal oligopyrimidine tract. *Oncogene* **2011**, *30*, 1531–1541. [[CrossRef](#)]
50. Schmied, W.H.; Tnimov, Z.; Uttamapinant, C.; Rae, C.D.; Fried, S.D.; Chin, J.W. Controlling orthogonal ribosome subunit interactions enables evolution of new function. *Nature* **2018**, *564*, 444–448. [[CrossRef](#)]

51. Woolford, J.L., Jr.; Baserga, S.J. Ribosome biogenesis in the yeast *Saccharomyces cerevisiae*. *Genetics* **2013**, *195*, 643–681. [[CrossRef](#)] [[PubMed](#)]
52. Bakshi, S.; Siryaporn, A.; Goulian, M.; Weisshaar, J.C. Superresolution imaging of ribosomes and RNA polymerase in live *Escherichia coli* cells. *Mol. Microbiol.* **2012**, *85*, 21–38. [[CrossRef](#)] [[PubMed](#)]
53. Klet, R.C.; Tussupbayev, S.; Borycz, J.; Gallagher, J.R.; Stalzer, M.M.; Miller, J.T.; Gagliardi, L.; Hupp, J.T.; Marks, T.J.; Cramer, C.J.; et al. Single-Site Organozirconium Catalyst Embedded in a Metal-Organic Framework. *J. Am. Chem. Soc.* **2015**, *137*, 15680–15683. [[CrossRef](#)] [[PubMed](#)]
54. Ji, P.; Solomon, J.B.; Lin, Z.; Johnson, A.; Jordan, R.F.; Lin, W. Transformation of Metal-Organic Framework Secondary Building Units into Hexanuclear Zr-Alkyl Catalysts for Ethylene Polymerization. *J. Am. Chem. Soc.* **2017**, *139*, 11325–11328. [[CrossRef](#)] [[PubMed](#)]
55. Canivet, J.; Aguado, S.; Schuurman, Y.; Farrusseng, D. MOF-supported selective ethylene dimerization single-site catalysts through one-pot postsynthetic modification. *J. Am. Chem. Soc.* **2013**, *135*, 4195–4198. [[CrossRef](#)]
56. Zhang, T.; Song, F.; Lin, W. Blocking bimolecular activation pathways leads to different regioselectivity in metal-organic framework catalysis. *Chem. Commun.* **2012**, *48*, 8766–8768. [[CrossRef](#)]
57. Mlinar, A.N.; Shylesh, S.; Ho, O.C.; Bell, A.T. Propene Oligomerization using Alkali Metal- and Nickel-Exchanged Mesoporous Aluminosilicate Catalysts. *ACS Catal.* **2013**, *4*, 337–343. [[CrossRef](#)]
58. Mlinar, A.N.; Keitz, B.K.; Gygi, D.; Bloch, E.D.; Long, J.R.; Bell, A.T. Selective Propene Oligomerization with Nickel(II)-Based Metal–Organic Frameworks. *ACS Catal.* **2014**, *4*, 717–721. [[CrossRef](#)]
59. Metzger, E.D.; Comito, R.J.; Hendon, C.H.; Dinca, M. Mechanism of Single-Site Molecule-Like Catalytic Ethylene Dimerization in Ni-MFU-4l. *J. Am. Chem. Soc.* **2017**, *139*, 757–762. [[CrossRef](#)]
60. Metzger, E.D.; Brozek, C.K.; Comito, R.J.; Dinca, M. Selective Dimerization of Ethylene to 1-Butene with a Porous Catalyst. *ACS Cent. Sci.* **2016**, *2*, 148–153. [[CrossRef](#)]
61. Finiels, A.; Fajula, F.; Hulea, V. Nickel-based solid catalysts for ethylene oligomerization—A review. *Catal. Sci. Technol.* **2014**, *4*, 2412–2426. [[CrossRef](#)]
62. Metzger, E.D.; Comito, R.J.; Wu, Z.; Zhang, G.; Dubey, R.C.; Xu, W.; Miller, J.T.; Dincă, M. Highly Selective Heterogeneous Ethylene Dimerization with a Scalable and Chemically Robust MOF Catalyst. *ACS Sustain. Chem. Eng.* **2019**, *7*, 6654–6661. [[CrossRef](#)]
63. Dubey, R.J.; Comito, R.J.; Wu, Z.; Zhang, G.; Rieth, A.J.; Hendon, C.H.; Miller, J.T.; Dinca, M. Highly Stereoselective Heterogeneous Diene Polymerization by Co-MFU-4l: A Single-Site Catalyst Prepared by Cation Exchange. *J. Am. Chem. Soc.* **2017**, *139*, 12664–12669. [[CrossRef](#)] [[PubMed](#)]
64. Comito, R.J.; Wu, Z.; Zhang, G.; Lawrence, J.A.; Korzynski, M.D., 3rd; Kehl, J.A.; Miller, J.T.; Dinca, M. Stabilized Vanadium Catalyst for Olefin Polymerization by Site Isolation in a Metal-Organic Framework. *Angew. Chem. Int. Ed. Engl.* **2018**, *57*, 8135–8139. [[CrossRef](#)] [[PubMed](#)]
65. Park, H.D.; Comito, R.J.; Wu, Z.; Zhang, G.; Ricke, N.; Sun, C.; Van Voorhis, T.; Miller, J.T.; Román-Leshkov, Y.; Dincă, M. Gas-Phase Ethylene Polymerization by Single-Site Cr Centers in a Metal–Organic Framework. *ACS Catal.* **2020**, *10*, 3864–3870. [[CrossRef](#)]
66. Vitorino, M.J.; Devic, T.; Tromp, M.; Férey, G.R.; Visseaux, M. Lanthanide Metal-Organic Frameworks as Ziegler-Natta Catalysts for the Selective Polymerization of Isoprene. *Macromol. Chem. Phys.* **2009**, *210*, 1923–1932. [[CrossRef](#)]
67. Rodrigues, I.; Mihalcea, I.; Volkringer, C.; Loiseau, T.; Visseaux, M. Water-free neodymium 2,6-naphthalenedicarboxylates coordination complexes and their application as catalysts for isoprene polymerization. *Inorg. Chem.* **2012**, *51*, 483–490. [[CrossRef](#)]
68. Russell, S.; Loiseau, T.; Volkringer, C.; Visseaux, M. Luminescent Lanthanide Metal Organic Frameworks for cis-Selective Isoprene Polymerization Catalysis. *Inorganics* **2015**, *3*, 467–481. [[CrossRef](#)]
69. Escribano, P.; Julián-López, B.; Planelles-Aragó, J.; Cordoncillo, E.; Viana, B.; Sanchez, C. Photonic and nanobiophotonic properties of luminescent lanthanide-doped hybrid organic–inorganic materials. *J. Mater. Chem.* **2008**, *18*, 23–40. [[CrossRef](#)]
70. Nguyen, H.L.; Gandara, F.; Furukawa, H.; Doan, T.L.; Cordova, K.E.; Yaghi, O.M. A Titanium-Organic Framework as an Exemplar of Combining the Chemistry of Metal- and Covalent-Organic Frameworks. *J. Am. Chem. Soc.* **2016**, *138*, 4330–4333. [[CrossRef](#)]

71. Nguyen, H.L.; Vu, T.T.; Le, D.; Doan, T.L.H.; Nguyen, V.Q.; Phan, N.T.S. A Titanium–Organic Framework: Engineering of the Band-Gap Energy for Photocatalytic Property Enhancement. *ACS Catal.* **2016**, *7*, 338–342. [[CrossRef](#)]
72. Lee, H.-C.; Antonietti, M.; Schmidt, B.V.K.J. A Cu(II) metal–organic framework as a recyclable catalyst for ARGET ATRP. *Polym. Chem.* **2016**, *7*, 7199–7203. [[CrossRef](#)]
73. Lee, H.-C.; Fantin, M.; Antonietti, M.; Matyjaszewski, K.; Schmidt, B.V.K.J. Synergic Effect between Nucleophilic Monomers and Cu(II) Metal–Organic Framework for Visible-Light-Triggered Controlled Photopolymerization. *Chem. Mater.* **2017**, *29*, 9445–9455. [[CrossRef](#)]
74. Marshall, N.; James, W.; Fulmer, J.; Crittenden, S.; Thompson, A.B.; Ward, P.A.; Rowe, G.T. Polythiophene Doping of the Cu-Based Metal–Organic Framework (MOF) HKUST-1 Using Innate MOF-Initiated Oxidative Polymerization. *Inorg. Chem.* **2019**, *58*, 5561–5575. [[CrossRef](#)] [[PubMed](#)]
75. Xing, H.; Chen, D.; Li, X.; Liu, Y.; Wang, C.; Su, Z. A visible-light responsive zirconium metal–organic framework for living photopolymerization of methacrylates. *RSC Adv.* **2016**, *6*, 66444–66450. [[CrossRef](#)]
76. Liu, Y.; Chen, D.; Li, X.; Yu, Z.; Xia, Q.; Liang, D.; Xing, H. Visible-light-induced controlled radical polymerization of methacrylates mediated by a pillared-layer metal–organic framework. *Green Chem.* **2016**, *18*, 1475–1481. [[CrossRef](#)]
77. Zhang, J.; Dumur, F.; Horcajada, P.; Livage, C.; Xiao, P.; Fouassier, J.P.; Gigmès, D.; Lalevée, J. Iron-Based Metal–Organic Frameworks (MOF) as Photocatalysts for Radical and Cationic Polymerizations under Near UV and Visible LEDs (385–405 nm). *Macromol. Chem. Phys.* **2016**, *217*, 2534–2540. [[CrossRef](#)]
78. Fu, Q.; Ranji-Burachaloo, H.; Liu, M.; McKenzie, T.G.; Tan, S.; Reyhani, A.; Nothling, M.D.; Dunstan, D.E.; Qiao, G.G. Controlled RAFT polymerization facilitated by a nanostructured enzyme mimic. *Polym. Chem.* **2018**, *9*, 4448–4454. [[CrossRef](#)]
79. Reyhani, A.; Ranji-Burachaloo, H.; McKenzie, T.G.; Fu, Q.; Qiao, G.G. Heterogeneously Catalyzed Fenton-Reversible Addition–Fragmentation Chain Transfer Polymerization in the Presence of Air. *Macromolecules* **2019**, *52*, 3278–3287. [[CrossRef](#)]
80. Arata, K. Organic syntheses catalyzed by superacidic metal oxides: Sulfated zirconia and related compounds. *Green Chem.* **2009**, *11*, 1719–1728. [[CrossRef](#)]
81. Trickett, C.A.; Osborn Popp, T.M.; Su, J.; Yan, C.; Weisberg, J.; Huq, A.; Urban, P.; Jiang, J.; Kalmutzki, M.J.; Liu, Q.; et al. Identification of the strong Bronsted acid site in a metal–organic framework solid acid catalyst. *Nat. Chem.* **2019**, *11*, 170–176. [[CrossRef](#)] [[PubMed](#)]
82. Liu, P.; Redekop, E.; Gao, X.; Liu, W.C.; Olsbye, U.; Somorjai, G.A. Oligomerization of Light Olefins Catalyzed by Bronsted-Acidic Metal–Organic Framework-808. *J. Am. Chem. Soc.* **2019**, *141*, 11557–11564. [[CrossRef](#)] [[PubMed](#)]
83. Ben, T.; Shi, K.; Cui, Y.; Pei, C.; Zuo, Y.; Guo, H.; Zhang, D.; Xu, J.; Deng, F.; Tian, Z.; et al. Targeted synthesis of an electroactive organic framework. *J. Mater. Chem.* **2011**, *21*, 3451–3479. [[CrossRef](#)]
84. Lu, C.; Ben, T.; Xu, S.; Qiu, S. Electrochemical synthesis of a microporous conductive polymer based on a metal–organic framework thin film. *Angew. Chem. Int. Ed. Engl.* **2014**, *53*, 6454–6458. [[CrossRef](#)] [[PubMed](#)]
85. Klyatskaya, S.; Kanj, A.B.; Molina-Jiron, C.; Heidrich, S.; Velasco, L.; Natzeck, C.; Gliemann, H.; Heissler, S.; Weidler, P.; Wenzel, W.; et al. Conductive Metal–Organic Framework Thin Film Hybrids by Electropolymerization of Monosubstituted Acetylenes. *ACS Appl. Mater. Interfaces* **2020**, *12*, 30972–30979. [[CrossRef](#)]
86. Jadhav, A.; Gupta, K.; Ninawe, P.; Ballav, N. Imparting Multifunctionality by Utilizing Biporosity in a Zirconium-Based Metal–Organic Framework. *Angew. Chem. Int. Ed. Engl.* **2020**, *59*, 2215–2219. [[CrossRef](#)]
87. Yanai, N.; Uemura, T.; Ohba, M.; Kadowaki, Y.; Maesato, M.; Takenaka, M.; Nishitsuji, S.; Hasegawa, H.; Kitagawa, S. Fabrication of two-dimensional polymer arrays: Template synthesis of polypyrrole between redox-active coordination nanoslits. *Angew. Chem. Int. Ed. Engl.* **2008**, *47*, 9883–9886. [[CrossRef](#)]
88. Le Ouay, B.; Boudot, M.; Kitao, T.; Yanagida, T.; Kitagawa, S.; Uemura, T. Nanostructuring of PEDOT in Porous Coordination Polymers for Tunable Porosity and Conductivity. *J. Am. Chem. Soc.* **2016**, *138*, 10088–10091. [[CrossRef](#)]
89. MacLean, M.W.; Kitao, T.; Suga, T.; Mizuno, M.; Seki, S.; Uemura, T.; Kitagawa, S. Unraveling Inter- and Intrachain Electronics in Polythiophene Assemblies Mediated by Coordination Nanospaces. *Angew. Chem. Int. Ed. Engl.* **2016**, *55*, 708–713. [[CrossRef](#)]

90. Kitao, T.; MacLean, M.W.A.; Le Ouay, B.; Sasaki, Y.; Tsujimoto, M.; Kitagawa, S.; Uemura, T. Preparation of polythiophene microrods with ordered chain alignment using nanoporous coordination template. *Polym. Chem.* **2017**, *8*, 5077–5081. [[CrossRef](#)]
91. Lee, H.-C.; Hwang, J.; Schilde, U.; Antonietti, M.; Matyjaszewski, K.; Schmidt, B.V.K.J. Toward Ultimate Control of Radical Polymerization: Functionalized Metal–Organic Frameworks as a Robust Environment for Metal-Catalyzed Polymerizations. *Chem. Mater.* **2018**, *30*, 2983–2994. [[CrossRef](#)]
92. Hwang, J.; Lee, H.-C.; Antonietti, M.; Schmidt, B.V.K.J. Free radical and RAFT polymerization of vinyl esters in metal–organic-frameworks. *Polym. Chem.* **2017**, *8*, 6204–6208. [[CrossRef](#)]
93. Zhang, Y.; Chen, D.; Guo, Z.; Wei, Z.; Zhang, X.; Xing, H. Visible-light-induced controlled radical polymerization of methacrylates mediated by zirconium-porphyrinic metal–organic frameworks. *New J. Chem.* **2020**, *44*, 5235–5242. [[CrossRef](#)]
94. Anan, S.; Mochizuki, Y.; Kokado, K.; Sada, K. Step-Growth Copolymerization Between an Immobilized Monomer and a Mobile Monomer in Metal-Organic Frameworks. *Angew. Chem. Int. Ed. Engl.* **2019**, *58*, 8018–8023. [[CrossRef](#)] [[PubMed](#)]
95. Kobayashi, Y.; Honjo, K.; Kitagawa, S.; Uemura, T. Preparation of Porous Polysaccharides Templated by Coordination Polymer with Three-Dimensional Nanochannels. *ACS Appl. Mater. Interfaces* **2017**, *9*, 11373–11379. [[CrossRef](#)]
96. Kitao, T.; Bracco, S.; Comotti, A.; Sozzani, P.; Naito, M.; Seki, S.; Uemura, T.; Kitagawa, S. Confinement of single polysilane chains in coordination nanospaces. *J. Am. Chem. Soc.* **2015**, *137*, 5231–5238. [[CrossRef](#)]
97. Distefano, G.; Suzuki, H.; Tsujimoto, M.; Isoda, S.; Bracco, S.; Comotti, A.; Sozzani, P.; Uemura, T.; Kitagawa, S. Highly ordered alignment of a vinyl polymer by host-guest cross-polymerization. *Nat. Chem.* **2013**, *5*, 335–341. [[CrossRef](#)]
98. Mochizuki, S.; Ogiwara, N.; Takayanagi, M.; Nagaoka, M.; Kitagawa, S.; Uemura, T. Sequence-regulated copolymerization based on periodic covalent positioning of monomers along one-dimensional nanochannels. *Nat. Commun.* **2018**, *9*, 329. [[CrossRef](#)]
99. Uemura, T.; Kitaura, R.; Ohta, Y.; Nagaoka, M.; Kitagawa, S. Nanochannel-promoted polymerization of substituted acetylenes in porous coordination polymers. *Angew. Chem. Int. Ed. Engl.* **2006**, *45*, 4112–4116. [[CrossRef](#)]
100. Uemura, T.; Hiramatsu, D.; Kubota, Y.; Takata, M.; Kitagawa, S. Topotactic linear radical polymerization of divinylbenzenes in porous coordination polymers. *Angew. Chem. Int. Ed. Engl.* **2007**, *46*, 4987–4990. [[CrossRef](#)]
101. Ling, J.J.J.; Policarpo, R.L.; Rabideau, A.E.; Liao, X.L.; Pentelute, B.L. Protein Thioester Synthesis Enabled by Sortase. *J. Am. Chem. Soc.* **2012**, *134*, 10749–10752. [[CrossRef](#)] [[PubMed](#)]
102. Uemura, T.; Nakanishi, R.; Kaseda, T.; Uchida, N.; Kitagawa, S. Controlled Cyclopolymerization of Difunctional Vinyl Monomers in Coordination Nanochannels. *Macromolecules* **2014**, *47*, 7321–7326. [[CrossRef](#)]
103. Kobayashi, Y.; Horie, Y.; Honjo, K.; Uemura, T.; Kitagawa, S. The controlled synthesis of polyglucose in one-dimensional coordination nanochannels. *Chem. Commun.* **2016**, *52*, 5156–5159. [[CrossRef](#)]
104. Rivera-Torrente, M.; Pletcher, P.D.; Jongkind, M.K.; Nikolopoulos, N.; Weckhuysen, B.M. Ethylene Polymerization over Metal–Organic Framework Crystallites and the Influence of Linkers on Their Fracturing Process. *ACS Catal.* **2019**, *9*, 3059–3069. [[CrossRef](#)]
105. Dong, Z.; Sun, Y.; Chu, J.; Zhang, X.; Deng, H. Multivariate Metal-Organic Frameworks for Dialing-in the Binding and Programming the Release of Drug Molecules. *J. Am. Chem. Soc.* **2017**, *139*, 14209–14216. [[CrossRef](#)]
106. Helal, A.; Yamani, Z.H.; Cordova, K.E.; Yaghi, O.M. Multivariate metal-organic frameworks. *Natl. Sci. Rev.* **2017**, *4*, 296–298. [[CrossRef](#)]
107. Ji, Z.; Li, T.; Yaghi, O.M. Sequencing of metals in multivariate metal-organic frameworks. *Science* **2020**, *369*, 674–780. [[CrossRef](#)]
108. Feng, L.; Yuan, S.; Li, J.L.; Wang, K.Y.; Day, G.S.; Zhang, P.; Wang, Y.; Zhou, H.C. Uncovering Two Principles of Multivariate Hierarchical Metal-Organic Framework Synthesis via Retrosynthetic Design. *ACS Cent. Sci.* **2018**, *4*, 1719–1726. [[CrossRef](#)]
109. Nath, I.; Chakraborty, J.; Verpoort, F. Metal organic frameworks mimicking natural enzymes: A structural and functional analogy. *Chem. Soc. Rev.* **2016**, *45*, 4127–4170. [[CrossRef](#)]

110. Wright, A.M.; Wu, Z.; Zhang, G.; Mancuso, J.L.; Comito, R.J.; Day, R.W.; Hendon, C.H.; Miller, J.T.; Dincă, M. A Structural Mimic of Carbonic Anhydrase in a Metal-Organic Framework. *Chem* **2018**, *4*, 2894–2901. [[CrossRef](#)]
111. Roberts, J.M.; Fini, B.M.; Sarjeant, A.A.; Farha, O.K.; Hupp, J.T.; Scheidt, K.A. Urea metal-organic frameworks as effective and size-selective hydrogen-bond catalysts. *J. Am. Chem. Soc.* **2012**, *134*, 3334–3337. [[CrossRef](#)] [[PubMed](#)]
112. McGuirk, C.M.; Katz, M.J.; Stern, C.L.; Sarjeant, A.A.; Hupp, J.T.; Farha, O.K.; Mirkin, C.A. Turning on catalysis: Incorporation of a hydrogen-bond-donating squaramide moiety into a Zr metal-organic framework. *J. Am. Chem. Soc.* **2015**, *137*, 919–925. [[CrossRef](#)] [[PubMed](#)]
113. Siu, P.W.; Brown, Z.J.; Farha, O.K.; Hupp, J.T.; Scheidt, K.A. A mixed dicarboxylate strut approach to enhancing catalytic activity of a de novo urea derivative of metal-organic framework UiO-67. *Chem. Commun.* **2013**, *49*, 10920–10922. [[CrossRef](#)] [[PubMed](#)]
114. Dong, X.W.; Liu, T.; Hu, Y.Z.; Liu, X.Y.; Che, C.M. Urea postmodified in a metal-organic framework as a catalytically active hydrogen-bond-donating heterogeneous catalyst. *Chem. Commun.* **2013**, *49*, 7681–7683. [[CrossRef](#)]
115. Katz, M.J.; Mondloch, J.E.; Totten, R.K.; Park, J.K.; Nguyen, S.T.; Farha, O.K.; Hupp, J.T. Simple and compelling biomimetic metal-organic framework catalyst for the degradation of nerve agent simulants. *Angew. Chem. Int. Ed. Engl.* **2014**, *53*, 497–501. [[CrossRef](#)]
116. Yang, X.L.; Wu, C.D. Metalloporphyrinic framework containing multiple pores for highly efficient and selective epoxidation. *Inorg. Chem.* **2014**, *53*, 4797–4799. [[CrossRef](#)]
117. Pullen, S.; Fei, H.; Orthaber, A.; Cohen, S.M.; Ott, S. Enhanced photochemical hydrogen production by a molecular diiron catalyst incorporated into a metal-organic framework. *J. Am. Chem. Soc.* **2013**, *135*, 16997–17003. [[CrossRef](#)]
118. Sasan, K.; Lin, Q.; Mao, C.; Feng, P. Incorporation of iron hydrogenase active sites into a highly stable metal-organic framework for photocatalytic hydrogen generation. *Chem. Commun.* **2014**, *50*, 10390–10393. [[CrossRef](#)]
119. Feng, Y.; Chen, C.; Liu, Z.; Fei, B.; Lin, P.; Li, Q.; Sun, S.; Du, S. Application of a Ni mercaptoprimidine MOF as highly efficient catalyst for sunlight-driven hydrogen generation. *J. Mater. Chem. A* **2015**, *3*, 7163–7169. [[CrossRef](#)]

Publisher's Note: MDPI stays neutral with regard to jurisdictional claims in published maps and institutional affiliations.



© 2020 by the authors. Licensee MDPI, Basel, Switzerland. This article is an open access article distributed under the terms and conditions of the Creative Commons Attribution (CC BY) license (<http://creativecommons.org/licenses/by/4.0/>).